

# On the Feasibility of Wireless Energy Transfer Based on Low Complexity Antenna Selection and Passive IRS Beamforming

Chandan Kumar<sup>ID</sup>, *Student Member, IEEE*, Salil Kashyap<sup>ID</sup>, *Member, IEEE*,  
Rimalapudi Sarvendranath<sup>ID</sup>, *Member, IEEE*, and Supreet Kumar Sharma<sup>ID</sup>

**Abstract**—We elucidate feasibility of wireless energy transfer (WET) with the help of an intelligent reflecting surface (IRS). We consider a source equipped with multiple antennas and a single radio-frequency (RF) chain. We propose a low complexity rule that does joint antenna selection (AS) at source and passive beamforming at IRS. We derive new expressions for probability of outage in WET under perfect and estimated channel knowledge and for both single and multiple users. We derive intuitive expressions for outage probability with large number of IRS elements and for line-of-sight scenarios. For a system with  $M$  antennas at source and  $N$  passive elements at IRS, we show that diversity order equals  $M + N$ . Extensions to subset AS, discrete phase-shift design, and performance under limited scattering are also presented. Our numerical results show that the proposed AS rule yields near-optimal performance while requiring only  $M + N$  pilot transmissions compared to the  $M + MN$  pilot transmissions required by the optimal AS rule in literature. We elucidate that we can trade-off active RF chains at source with passive elements at IRS to obtain improved performance both in terms of outage probability and power transfer efficiency. And 3-bit IRS is sufficient to obtain good performance at lower complexity.

**Index Terms**—Wireless energy transfer, IRS, outage probability, antenna selection, channel estimation.

## I. INTRODUCTION

IT is predicted that an exceptionally large number of Internet-of-things (IoT) devices will be part of the cellular network in the next five years [1]. These IoT devices include sensors that sense data and communicate over a network. They find wide applications in consumer electronics, intelligent transportation, telecommunications, smart grids, home automation, intrusion detection for security, and autonomous monitoring of health, environment and structures. They usually

operate on limited capacity batteries. Hence, their batteries need to be replaced or recharged from time-to-time for continued operation. This may not be feasible when these devices are placed in hazardous or inaccessible locations.

Wireless energy transfer (WET), in which these energy-constrained devices harvest energy from electromagnetic signals, helps in charging the batteries of these massive number of IoT devices [2]. However, we need to address several new design challenges in order to enable WET. Firstly, a very small percentage of the power radiated by a source is harvested by a device due to severe path loss and limitations of the harvesting circuitry. Secondly, design of WET systems must ensure that the sensors harvest more energy than what they consume to sense, compute, and communicate. Thirdly, the receive power levels that are sufficient for reliable data transfer and decoding are not sufficient for activating the harvester in these sensors.

It is shown that WET is feasible with massive antenna arrays [3], [4]. However, these systems need a radio-frequency (RF) chain for each antenna and consume large amount of power. Intelligent reflecting surface (IRS), which uses an array of passive low-cost reflecting elements, is shown to enable WET [5], [6]. Furthermore, it has the potential to boost spectral and energy efficiencies, security and coverage of a wireless network. It is being envisioned as a promising 6G technology [7], [8]. Each of the passive IRS elements can be programmed to induce a known amplitude and phase shift to the incident signal. Programming these low cost passive elements to ensure coherent combination of signals at the receiver improves the receive signal energy. It thus enhances reliability and enables wireless charging.

### A. Related Literature

We now present some key related references below.

1) *IRS-Assisted WET System*: The authors in [5] proposed a channel estimation protocol and designed near-optimal beamformers at base station (BS) and at IRS. Active beamformer at BS and constant envelope precoding based passive beamformer at IRS were designed to maximize sum received power at IoT users [6]. Average symbol error and outage probabilities were derived with perfect channel state information (CSI) in [9]. The authors in [10] designed active beamforming at source and passive beamforming at IRS to maximize minimum harvested power among users. In [11], the authors jointly

Manuscript received 26 March 2022; accepted 27 May 2022. Date of publication 8 June 2022; date of current version 16 August 2022. This work was supported by the Science and Engineering Research Board (SERB) under Grant CRG/2021/001816. The associate editor coordinating the review of this article and approving it for publication was X. Chen. (*Corresponding author: Chandan Kumar.*)

Chandan Kumar, Salil Kashyap, and Rimalapudi Sarvendranath are with the Department of Electronics and Electrical Engineering (EEE), IIT Guwahati, Guwahati 781039, India (e-mail: rabishchandan@gmail.com; salilkashyap@gmail.com; sarvendranath@gmail.com).

Supreet Kumar Sharma is with Mavenir Systems Pvt. Ltd., Bengaluru 560045, India (e-mail: supreet023@gmail.com).

Digital Object Identifier 10.1109/TCOMM.2022.3181056

0090-6778 © 2022 IEEE. Personal use is permitted, but republication/redistribution requires IEEE permission.  
See <https://www.ieee.org/publications/rights/index.html> for more information.

optimized beamformers at the source and at the IRS to maximize the total power received by the users. The authors in [12] maximized weighted sum direct current under a transmit power constraint at source and unit modulus constraint at IRS.

2) *IRS-Assisted Simultaneous Wireless Information and Power Transfer System*: The authors in [13] maximized the common throughput of the information and energy users by jointly optimizing transmit time, power allocation, and reflection coefficients at IRS. In [14], the authors jointly optimized beamformer at the BS and transmission mode at the IRS to minimize total BS transmit power. In [15], the authors designed active beamforming at the BS and phase shifts at the IRS to minimize transmit power under signal to interference plus noise ratio constraint at the information user and energy harvesting constraint at the energy user. In [16], the authors determined the optimal power splitting ratio, active beamforming at the BS, and phase shifts of the IRS to maximize the energy efficiency.

Based on the discussion above, we observe that most of the works considered IRS assisted transmission from a source that is equipped with as many RF chains as the number of antennas. This increases hardware complexity, power consumption and cost at the source. Antenna selection (AS) is a low complexity technique that reduces the cost and power consumption at the source. There are limited works available on joint AS-IRS beamforming. While [17] studied joint AS at the BS and passive beamforming at the IRS to maximize received signal power under perfect CSI. The authors in [18] considered joint AS and IRS beamforming to maximize the ergodic sum data rate and in [19], algorithms were developed for joint AS and passive beamforming at the IRS to maximize channel capacity under unit modulus constraints of all IRS elements assuming perfect CSI. However, system modeling, developing low complexity AS rule, active and passive beamforming design based on the selected antennas, and comprehensive performance analysis under both perfect and estimated CSI for joint AS and IRS-assisted WET to single and/or multiple users is still in its infancy, remains an open problem and is the focus of this work.

### B. Focus and Contributions

We consider a practically relevant model where a source equipped with fewer RF chains than the number of transmit antennas is assisted by an IRS to transfer energy wirelessly. Each transmit RF chain, which is made up of digital-to-analog converters, up-converters, filters, and power amplifiers makes the source power hungry, bulky and costly. AS employed by source reduces the number of RF chains required, thus reducing hardware complexity, power consumption, and the associated cost. For this model, our main objective is to ascertain whether the receive power level at the user can be maintained at the same level by trading-off active RF chains at the source with passive elements at the IRS that do not require dedicated RF chains. Our model includes as a special case, the full-complexity system in which the source is equipped with as many RF chains as the number of antennas. We next summarize our key contributions:

- *AS Rule*: For a system with  $M$  antennas at source and  $N$  passive elements at IRS, we propose a joint AS and passive beamforming rule that requires only  $M + N$  pilot transmissions for channel estimation. This is significantly lower than  $M + MN$  pilot transmissions required by the optimal rule in [17], [18]. Therefore, the proposed AS rule reduces the pilot transmissions significantly and increases the time available for WET.
- *Performance Analysis*: We derive new analytical expression for probability of outage<sup>1</sup> in WET with perfect CSI. We also derive new expressions for minimum number of IRS elements required to avoid outage. These provide key insights related to WET system design.
- *Estimated CSI*: We also derive a novel mathematical expression that approximates the probability of outage in WET with minimum mean square error (MMSE) estimate of the cascaded and the direct channels. Our analysis helps in understanding the robustness of WET in practical scenarios in which the channel estimates are likely to be imperfect. The analysis involves order statistics of the magnitude of the estimated direct path channel gains and depends on IRS phase-shifts that are designed based on estimated CSI.
- *Diversity Order*: We prove that diversity order of a joint AS and IRS assisted WET is equal to sum of the number of transmit antennas and number of IRS elements, i.e.,  $M + N$ .
- *Subset AS*: We next generalize our model to include a source that is equipped with more than one RF chain and selects a subset of antennas based on strength of the direct channels to the user. We apply alternating optimization to obtain the beamformer at the source and phase-shifts at the IRS. And elucidate the trade-off between probability of outage in WET and power transfer efficiency (PTE) under AS and full-complexity based energy beamforming.
- *Discrete Phase Shifts*: We then study impact of practically relevant and implementation-friendly discrete phase shift design at IRS on performance. We show that a 3-bit programmable IRS is sufficient to achieve good trade-off between complexity and performance.
- *Multi-User Scenario*: We derive novel analytical bounds on probability of outage in WET to multiple users under both perfect and estimated CSI, where users are served based on round-robin scheduling strategy. This analysis takes into account the correlation arising due to common source to IRS links for different users.
- *Limited Scattering*: We also study impact of limited number of scatterers and inter-element spacing on the outage probability [23]. We show how by exploiting the underlying spatial correlation, the pilot overhead can be reduced further from  $M + N$  to  $M + \frac{N}{G}$ , where  $G$

<sup>1</sup>This is an appropriate performance metric to ascertain feasibility of WET in a wireless system with static or limited mobility users [3], [4], [20]–[22]. It helps identify operational regimes where users harvest more than what they consume in tasks related to channel estimation, sensing, computation, and communication.

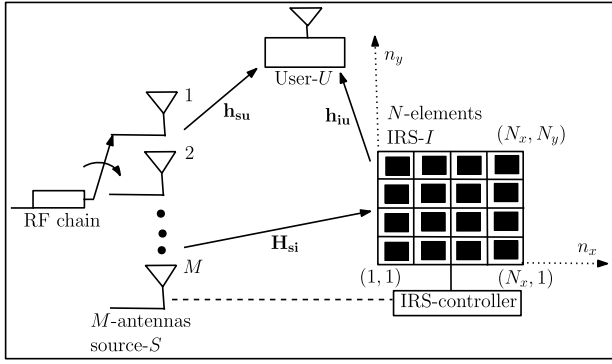


Fig. 1. System model: Joint AS and IRS-assisted WET.

denotes number of adjacent IRS elements configured with identical phase-shifts.

*Notations:* Boldface uppercase and lowercase letters denote matrices and vectors, respectively. The expectation and variance operators are denoted by  $\mathbb{E}(\cdot)$  and  $\text{var}(\cdot)$ , respectively. A complex Gaussian random variable (RV)  $X$  with mean  $\mu$  and variance  $\sigma^2$  is denoted as  $X \sim \mathcal{CN}(\mu, \sigma^2)$ . We denote an  $N \times N$  diagonal matrix with diagonal elements  $a_1, \dots, a_N$  by  $(a_1, \dots, a_N)$ . The probability of an event  $A$  is denoted by  $\Pr(A)$  and probability density function (pdf) of a RV  $X$  is denoted by  $f_X(\cdot)$ . Real and imaginary parts of a complex variable are denoted by  $\Re(\cdot)$  and  $\Im(\cdot)$ , respectively.

*Organization:* The paper is organized as follows. We present the system model in Section II. We propose our joint AS and passive beamforming rule, analyze its probability of outage with perfect CSI and extend this analysis to multi-user scenario in Section III. We analyze the corresponding performance with estimated CSI in Section IV. The numerical results and conclusions are presented in Sections V and VI, respectively.

## II. SYSTEM MODEL

We consider an IRS-assisted WET system as shown in Figure 1. It has a source  $S$  equipped with  $M$  antennas and a single RF chain that transmits RF signal to a single antenna user  $U$ . We consider that the passive reflecting elements of IRS  $I$  are arranged in a planar array of dimension  $N_x \times N_y$ , where  $N_x$  and  $N_y$  denote the number of IRS elements along length and breadth, respectively. Therefore, total number of IRS elements  $N = N_x N_y$ . The source dynamically switches its RF chain to the antenna selected based on instantaneous CSI. It also computes the IRS reflection coefficients, which are communicated to IRS through a dedicated control link. We consider a block fading model, in which the wireless channel remains constant over a coherence interval of duration  $\tau_c$  and varies independently across different coherence intervals. We consider time division duplex (TDD)<sup>2</sup> mode of communication to exploit channel reciprocity. The CSI acquired through uplink (UL) pilot signaling is used to select an antenna at  $S$  and compute reflection coefficients at  $I$ .

<sup>2</sup>Indoor/outdoor field trials confirmed that UL and downlink (DL) channels are reciprocal in TDD mode even in IRS-aided wireless communications [24]. Furthermore, this has been widely adopted in literature [5], [25]–[28].

We consider that the IRS is completely passive in nature and does not have dedicated RF chains connected to it. Let  $\mathbf{h}_{su} \in \mathcal{C}^{M \times 1}$  denote the complex channel gain vector of direct path from  $S$  to  $U$ . We model it as Rayleigh fading. Therefore,  $\mathbf{h}_{su} \sim \mathcal{CN}(\mathbf{0}, \beta_{su} \mathbf{I}_M)$ , where  $\beta_{su}$  denotes distance-dependent path loss. Let  $\mathbf{H}_{si} \in \mathcal{C}^{M \times N}$  denote complex channel gain matrix from  $S$  to  $I$ . We model it as Rician fading. It can be written as

$$\mathbf{H}_{si} = \sqrt{\frac{K_{si} \zeta_{si}}{K_{si} + 1}} \bar{\mathbf{H}}_{si} + \sqrt{\frac{\zeta_{si}}{K_{si} + 1}} \tilde{\mathbf{H}}_{si}, \quad (1)$$

where  $\zeta_{si}$  and  $K_{si}$  denote the distance-dependent path loss and the Rician factor, respectively. Furthermore, the  $(m, n)$ <sup>th</sup> element of the line-of-sight (LoS) component  $\bar{\mathbf{H}}_{si} \in \mathcal{C}^{M \times N}$  is given by  $\bar{H}_{si}^{mn} = \exp[j \frac{2\pi}{\lambda} d ((m-1) \sin(\psi_1) \cos(\phi_1) + (n_x-1) \sin(\psi_2) \cos(\phi_2) + (n_y-1) \sin(\psi_2) \sin(\phi_2))]$ , where the index  $n = (n_x - 1) + 1 + (n_y - 1) N_x$ ,  $\lambda$  denotes the wavelength,  $d$  denotes the inter-element spacing at  $S$  and  $I$ ,  $\psi_1, \phi_1, \psi_2, \phi_2 \in (0, 2\pi)$  denote the elevation angle of departure (AoD) and azimuthal AoD at  $S$ , elevation angle of arrival (AoA), and azimuthal AoA at  $I$ , respectively,  $1 \leq m \leq M$ ,  $1 \leq n_x \leq N_x$ , and  $1 \leq n_y \leq N_y$  [23]. The elements of the non-LoS component  $\tilde{\mathbf{H}}_{si} \in \mathcal{C}^{M \times N}$  are independent and identically distributed (i.i.d.) circular symmetric complex Gaussian RVs with zero mean and unit variance, i.e.,  $\tilde{H}_{si}^{mn} \sim \mathcal{CN}(0, 1)$ . Thus,  $H_{si}^{mn} \sim \mathcal{CN}(\mu_{si}^{mn}, \beta_{si})$ , where  $\mu_{si}^{mn} = \sqrt{\frac{K_{si} \zeta_{si}}{K_{si} + 1}} \bar{H}_{si}^{mn}$  and  $\beta_{si} = \frac{\zeta_{si}}{K_{si} + 1}$ . The elements of the channel matrix  $\mathbf{H}_{si}$  are independent across  $m$  and  $n$ .

Let  $\mathbf{h}_{iu} \in \mathcal{C}^{N \times 1}$  denote the complex channel gain vector from  $I$  to  $U$ . It is modeled as

$$\mathbf{h}_{iu} = \sqrt{\frac{K_{iu} \zeta_{iu}}{K_{iu} + 1}} \bar{\mathbf{h}}_{iu} + \sqrt{\frac{\zeta_{iu}}{K_{iu} + 1}} \tilde{\mathbf{h}}_{iu}, \quad (2)$$

where  $\zeta_{iu}$  and  $K_{iu}$  denote the distance-dependent path loss and the Rician factor, respectively. The  $n$ <sup>th</sup> element of the LoS component  $\bar{\mathbf{h}}_{iu} \in \mathcal{C}^{N \times 1}$  is given by  $\bar{h}_{iu}^n = \exp[j \frac{2\pi}{\lambda} d ((n_x-1) \sin(\psi_3) \cos(\phi_3) + (n_y-1) \sin(\psi_3) \cos(\phi_3))]$ , where  $\psi_3, \phi_3 \in (0, 2\pi)$  denote the elevation AoD and azimuthal AoD at  $I$ , respectively [23]. Furthermore,  $\tilde{\mathbf{h}}_{iu} \in \mathcal{C}^{N \times 1}$  denotes the non-LoS component with i.i.d.  $\mathcal{CN}(0, 1)$  elements. Thus,  $h_{iu}^n \sim \mathcal{CN}(\mu_{iu}^n, \beta_{iu})$ , where  $\mu_{iu}^n = \sqrt{\frac{K_{iu} \zeta_{iu}}{K_{iu} + 1}} \bar{h}_{iu}^n$  and  $\beta_{iu} = \frac{\zeta_{iu}}{K_{iu} + 1}$ . The elements of the channel vector  $\mathbf{h}_{iu}$  are independent of each other. Let  $\alpha_n \in [0, 1]$  and  $\theta_n \in [0, 2\pi]$  denote the amplitude and phase coefficients of the  $n$ <sup>th</sup> IRS element. Then, the phase shift matrix of the IRS is given by  $\Theta = (\alpha_1 e^{j\theta_1}, \alpha_2 e^{j\theta_2}, \dots, \alpha_N e^{j\theta_N})$ .

Let  $a \in \{1, 2, \dots, M\}$  denote the index of the antenna selected at  $S$ . Furthermore, let  $\mathbf{h}_{su}^a$  and  $\mathbf{h}_{si}^a \in \mathcal{C}^{1 \times N}$  denote  $a$ <sup>th</sup> element of  $\mathbf{h}_{su}$  and  $a$ <sup>th</sup> row of  $\mathbf{H}_{si}$ , respectively. Then, the DL signal received at the user is given by

$$y_u = (\mathbf{h}_{su}^a + \mathbf{h}_{si}^a \Theta \mathbf{h}_{iu}) x_s + w_u, \quad (3)$$

where  $x_s$  denotes the transmit symbol and  $w_u$  denotes circular symmetric complex additive white Gaussian noise (AWGN) with variance  $\sigma^2$ . Therefore,  $w_u \sim \mathcal{CN}(0, \sigma^2)$ .

Let  $\mathbf{g}_{s_{iu}}^a = [g_{s_{iu}}^{a1}, \dots, g_{s_{iu}}^{aN}] = \mathbf{h}_{s_i}^a(\mathbf{h}_{i_u}^T) \in \mathcal{C}^{1 \times N}$  denote the vector of cascaded channels of the reflected path. Furthermore, let  $\mathbf{f}_i = [f_i^1, \dots, f_i^N]^T$  denote the IRS passive beamforming vector, where  $f_i^n$  denotes the  $n^{\text{th}}$  diagonal element of  $\Theta$  and is given by  $f_i^n = \alpha_n e^{j\theta_n}$ . Using these notations, the signal  $y_u$  in (3) can be re-written as

$$y_u = (h_{su}^a + \mathbf{g}_{s_{iu}}^a \mathbf{f}_i) x_s + w_u. \quad (4)$$

### III. AS RULE AND ITS ANALYSIS WITH PERFECT CSI

In this section, we state our low-complexity AS rule and derive its outage probability with perfect CSI.<sup>3</sup> Let  $\rho_{su}^m$  and  $\Lambda_{su}^m$  denote the magnitude and phase of the direct path channel gain  $h_{su}^m$ , i.e.,  $h_{su}^m = \rho_{su}^m e^{j\Lambda_{su}^m}$ , for  $m \in \{1, 2, \dots, M\}$ .

#### A. AS and Passive Beamforming

The source selects the antenna with the highest channel power gain along the direct path from  $S$  to  $U$ . Therefore,  $a = \arg \max_{m \in \{1, 2, \dots, M\}} \{\rho_{su}^m\}$ . From  $y_u$  in (4), the energy harvested at  $U$  in a coherence interval of duration  $\tau_c$  seconds is given by

$$\begin{aligned} E_u &= \eta_r \tau_c |x_s|^2 |h_{su}^a + \mathbf{g}_{s_{iu}}^a \mathbf{f}_i|^2 \\ &= \eta_r \tau_c |x_s|^2 \left| h_{su}^a + \sum_{n=1}^N g_{s_{iu}}^{an} f_i^n \right|^2, \end{aligned} \quad (5)$$

where  $0 < \eta_r < 1$  denotes the rectification efficiency of the energy harvesting circuit at the user.<sup>4</sup> Let  $p = |x_s|^2$  and  $\gamma = \eta_r \tau_c p$ . The contribution of noise  $w_u$  to the harvested energy is negligibly small and is therefore not considered [3]–[6], [31]. In terms of magnitude and phase, we can express the RVs in (5) as  $g_{s_{iu}}^{an} = \rho_{s_{iu}}^{an} e^{j\phi_{s_{iu}}^{an}}$ , where  $\rho_{s_{iu}}^{an} = \rho_{s_i}^{an} \rho_{i_u}^n$ ,  $\rho_{s_i}^{an} = |H_{s_i}^{an}|$ ,  $\rho_{i_u}^n = |h_{i_u}^n|$  and  $\phi_{s_{iu}}^{an} = \angle H_{s_i}^{an} + \angle h_{i_u}^n$ . Therefore,  $E_u$  in (5) can be expressed as

$$E_u = \gamma \left| \rho_{su}^a e^{j\Lambda_{su}^a} + \sum_{n=1}^N \rho_{s_{iu}}^{an} e^{j\phi_{s_{iu}}^{an}} f_i^n \right|^2. \quad (6)$$

By triangle inequality, we know that programming  $f_i^n = e^{-j(\phi_{s_{iu}}^{an} - \Lambda_{su}^a)}$  maximizes  $E_u$  in (6). This choice enables coherent combination of the direct path signal and the reflected path signals via the IRS. Therefore, our joint AS and passive beamforming rule can be written as

$$a = \arg \max_{m \in \{1, 2, \dots, M\}} \{\rho_{su}^m\}, \quad (7)$$

$$f_i^n = \exp(-j(\phi_{s_{iu}}^{an} - \Lambda_{su}^a)), \quad \text{for } n = 1, \dots, N. \quad (8)$$

We now describe the two-step procedure that implements the above AS rule. *Step 1:* The IRS is turned off and the user sends  $M$  pilots. The source estimates the direct path CSI and selects antenna  $a$  in (7). *Step 2:* The source switches the RF

<sup>3</sup>WET with perfect CSI refers to genie-aided WET, where the CSI is error-free and no resources are spent on pilots.

<sup>4</sup>With a single energy harvesting circuit, the energy harvested is a non-linear function of the received energy due to saturation effects. However, it is shown that we can mitigate the non-linear behavior and also extend the range over which it is a linear function by using multiple such circuits in parallel [13], [29], [30].

chain to the selected antenna and the IRS is turned on. Now the user sends  $N$  pilots and the source estimates the sum of direct path and the reflected path CSI corresponding to the antenna  $a$  selected. Then, the source subtracts the direct path CSI to obtain the reflected path CSI and computes the IRS passive beamforming coefficients as in (8). These coefficients are communicated to the IRS through the dedicated control link. The channel estimation procedure in these two steps is discussed in detail in Section IV-A.

*Benefits of the Proposed Rule:* (i) It reduces number of pilot transmissions required and increases the time available for WET. Based on the above description, we see that the proposed joint AS and passive beamforming rule requires  $M + N$  pilots to obtain required CSI. This is significantly lower than the  $M + MN$  pilots required by the optimal AS rule proposed in [17], [18]. (ii) In Section V, we show that the proposed rule is near-optimal with fewer pilots. (iii) Furthermore, it simplifies outage analysis and brings out valuable insights.

#### B. Probability of Outage Analysis

Let  $E_{\text{th}}$  denote the threshold energy required at the user. We now derive an expression for the probability of outage in WET, i.e.,  $\Pr(E_u \leq E_{\text{th}})$ , for the proposed joint AS and passive beamforming rule with perfect CSI. Substituting  $f_i^n$  from (8) in (6), we get

$$E_u = \gamma \left( \rho_{su}^a + \sum_{n=1}^N \rho_{s_{iu}}^{an} \right)^2. \quad (9)$$

Here,  $E_u$  is square of the sum of two independent RVs  $\rho_{su}^a$  and  $\sum_{n=1}^N \rho_{s_{iu}}^{an}$ . From (7), we know that  $\rho_{su}^a = \max\{\rho_{su}^1, \dots, \rho_{su}^M\}$ , which is the maximum of  $M$  i.i.d. Rayleigh RVs. Furthermore,  $\sum_{n=1}^N \rho_{s_{iu}}^{an} = \sum_{n=1}^N \rho_{s_i}^{an} \rho_{i_u}^n$  is the sum of the product of independent Rician RVs. Therefore, the probability of outage in energy transfer can be written as

$$P_{\text{outage}} = \Pr(E_u \leq E_{\text{th}}) = \Pr \left( \gamma \left( \rho_{su}^a + \sum_{n=1}^N \rho_{s_{iu}}^{an} \right)^2 \leq E_{\text{th}} \right). \quad (10)$$

*Theorem 1:* The probability of outage for the proposed joint AS and passive beamforming rule with perfect CSI is given by

$$\begin{aligned} P_{\text{outage}} &= \sum_{m=0}^{M-1} \frac{M(-1)^m (M-1)}{m+1} \binom{M-1}{m} \left[ 1 - \psi Q \left( \frac{\bar{E}_{\text{th}} - \mu_y}{\sigma_y} \right) \right. \\ &\quad \left. - \frac{\psi e^{\frac{\xi^2 - \eta \chi}{2\eta}}}{\sqrt{\eta \sigma_y^2}} \left( Q \left( \frac{-\xi}{\sqrt{\eta}} \right) - Q \left( \frac{\bar{E}_{\text{th}} - \mu_y}{\sigma_y \sqrt{\eta}} \right) \right) \right], \end{aligned} \quad (11)$$

where  $\psi = Q^{-1} \left( \frac{-\mu_y}{\sigma_y} \right)$ ,  $\eta = \left( \frac{2(m+1)}{\beta_{su}} + \frac{1}{\sigma_y^2} \right)$ ,  $\xi = \left( \frac{2(m+1)\bar{E}_{\text{th}}}{\beta_{su}} + \frac{\mu_y}{\sigma_y^2} \right)$ ,  $\chi = \left( \frac{2(m+1)\bar{E}_{\text{th}}}{\beta_{su}} + \frac{\mu_y}{\sigma_y^2} \right)$ ,  $\bar{E}_{\text{th}} = \sqrt{\frac{E_{\text{th}}}{\gamma}}$ ,  $\mu_y = \frac{N\pi}{4} \sqrt{\beta_{si}\beta_{iu}} L_{\frac{1}{2}}(-K_{si}) L_{\frac{1}{2}}(-K_{iu})$ ,  $\sigma_y^2 = N\beta_{si}\beta_{iu} (1 + K_{si})(1 + K_{iu}) - N\mu_0^2$ ,  $\mu_0 =$

$\frac{\pi}{4}\sqrt{\beta_{si}\beta_{iu}}L_{\frac{1}{2}}(-K_{si})L_{\frac{1}{2}}(-K_{iu})$ ,  $Q(\cdot)$  denotes the Q-function [32] and  $L_n(\cdot)$  denotes Laguerre polynomial of order- $n$  [33].

*Proof:* The proof is given in Appendix A. ■

The above expression brings out the dependence of the probability of outage on system parameters  $M$ ,  $N$ , and  $E_{th}$  and channel parameters  $K_{si}$ ,  $K_{iu}$ ,  $\beta_{su}$ ,  $\beta_{si}$  and  $\beta_{iu}$ . With  $M = 1$ ,  $P_{outage}$  in (11) reduces to a form similar to [34, Eqn. (7)].

1) *Asymptotic Analysis:* We now study the behavior of the probability of outage for large number of IRS elements. As  $N \rightarrow \infty$ , by law of large numbers [35], we know that  $\frac{1}{N} \sum_{n=1}^N \rho_{siu}^{an} \rightarrow \mathbb{E}(\rho_{siu}^{an}) = \mathbb{E}(\rho_{si}^{an})\mathbb{E}(\rho_{iu}^{an}) = \mu_0 = \frac{\pi}{4}\sqrt{\beta_{si}\beta_{iu}}L_{\frac{1}{2}}(-K_{si})L_{\frac{1}{2}}(-K_{iu})$ . Furthermore, the outage event can be written as  $\left(\frac{1}{N}\rho_{su}^a + \frac{1}{N} \sum_{n=1}^N \rho_{siu}^{an} \leq \frac{1}{N}\bar{E}_{th}\right)$ . For sufficiently large  $N$ ,  $\frac{1}{N} \sum_{n=1}^N \rho_{siu}^{an} \rightarrow \mu_0$  and

$$P_{outage} \rightarrow \Pr(\rho_{su}^a \leq \bar{E}_{th} - N\mu_0). \quad (12)$$

Using the fact that  $\rho_{su}^a = \max\{\rho_{su}^1, \dots, \rho_{su}^M\}$ , the outage probability

$$P_{outage} \rightarrow \Pr(\rho_{su}^1 \leq \bar{E}_{th} - N\mu_0, \dots, \rho_{su}^M \leq \bar{E}_{th} - N\mu_0). \quad (13)$$

Since  $\rho_{su}^1, \dots, \rho_{su}^M$  are i.i.d. Rayleigh RVs, we get

$$P_{outage} \rightarrow \begin{cases} 0, & \text{If } N\mu_0 \geq \bar{E}_{th}, \\ \left[1 - \exp\left(-\frac{(\bar{E}_{th} - N\mu_0)^2}{\beta_{su}}\right)\right]^M, & \text{Otherwise.} \end{cases} \quad (14)$$

From the analysis above, we see that  $P_{outage} \rightarrow 0$  when  $N\mu_0 \geq \bar{E}_{th}$ . Therefore, the probability of outage can be made negligibly small when the number of IRS elements is greater than

$$\frac{4\sqrt{\bar{E}_{th}}}{\pi\sqrt{p\eta_r\tau_c}\sqrt{\beta_{si}\beta_{iu}}L_{\frac{1}{2}}(-K_{si})L_{\frac{1}{2}}(-K_{iu})}. \quad (15)$$

*Insights:* We see that the minimum number of IRS elements required is inversely proportional to the strength of the cascaded reflected path. It decreases as the strength of the LoS components increases, i.e., as  $K_{si}$  or  $K_{iu}$  increases. This is because  $L_{\frac{1}{2}}(x)$  is a monotonically decreasing function of  $x$ . Furthermore, it is independent of the strength of the direct path.

2) *LoS Scenario:* We now consider a special case when there are only LoS components from  $S \rightarrow I$  and from  $I \rightarrow U$ , i.e.,  $K_{si} \rightarrow \infty$  and  $K_{iu} \rightarrow \infty$ . Therefore,  $\mathbf{H}_{si} = \sqrt{\zeta_{si}} \bar{\mathbf{H}}_{si}$  and  $\mathbf{h}_{iu} = \sqrt{\zeta_{iu}} \bar{\mathbf{h}}_{iu}$ . In this case,  $\sum_{n=1}^N \rho_{siu}^{an} = N\sqrt{\zeta_{si}\zeta_{iu}}$  and the probability of outage in (10) reduces to

$\Pr(\rho_{su}^a \leq \bar{E}_{th} - N\sqrt{\zeta_{si}\zeta_{iu}})$ . Further simplification yields

$$P_{outage} = \begin{cases} 0, & \text{If } N\sqrt{\zeta_{si}\zeta_{iu}} \geq \bar{E}_{th}, \\ \left[1 - \exp\left(-\frac{(\bar{E}_{th} - N\sqrt{\zeta_{si}\zeta_{iu}})^2}{\beta_{su}}\right)\right]^M, & \text{Otherwise.} \end{cases} \quad (16)$$

Note that (16) is an exact expression for the probability of outage in WET. Here, employing  $\sqrt{\bar{E}_{th}/(p\eta_r\tau_c\zeta_{si}\zeta_{iu})}$  number of IRS elements will yield zero outage probability.

3) *Extension to Multi-User Scenario:* With  $K$  users, if the source transmits energy wirelessly to every user based on round-robin scheduling strategy over a slot of length  $\frac{\tau_c}{K}$  seconds, then the joint AS and passive beamforming rule is given by  $a_k = \arg \max_{m \in \{1, 2, \dots, M\}} \{\rho_{sk}^m\}$  and  $f_{ik}^n = \exp(-j(\phi_{sik}^{a_k n} - \Lambda_{sk}^{a_k}))$ , for  $n = 1, \dots, N$ , where  $1 \leq k \leq K$  denotes index of the user being served in slot  $k$ ,  $\rho_{sk}^m$  denotes magnitude of the direct path channel gain from the  $m^{\text{th}}$  antenna at the source to user  $k$ ,  $\Lambda_{sk}^{a_k}$  denotes phase of the direct path channel gain from the selected antenna  $a_k$  at the source to user  $k$  and  $\phi_{sik}^{a_k n} = \angle H_{si}^{a_k n} + \angle h_{ik}^n$ . Note that  $\angle H_{si}^{a_k n}$  denotes the phase of the channel between the selected antenna  $a_k$  at  $S$  and  $n^{\text{th}}$  IRS element and  $\angle h_{ik}^n$  denotes phase of the channel between  $n^{\text{th}}$  IRS element and  $k^{\text{th}}$  user. For this model,  $P_{outage}$  equals one minus the probability that every user harvests more than  $E_{th}$  amount of energy. Mathematically,  $P_{outage} = 1 - \Pr\left(\bigcap_{k=1}^K E_k > E_{th}\right)$ , where  $E_k$  denotes energy harvested by  $k^{\text{th}}$  user.

*Theorem 2:* An upper bound on probability of outage in WET with perfect CSI when users are served based on round-robin scheduling strategy is given by

$$P_{outage} \leq \min\left(1, \sum_{k=1}^K \Pr(E_k \leq E_{th})\right), \quad (17)$$

where  $\Pr(E_k \leq E_{th})$  is given in Theorem 1 with  $\gamma$  replaced by  $\frac{\gamma}{K}$ .

*Proof:* For  $1 \leq k \leq K$ , the events  $\{E_k > E_{th}\}$  are not mutually independent. This is because the channel between source and IRS for different users may be exactly the same if source ends up selecting the same antenna for different users. Therefore, using Boole-Fréchet inequality,<sup>5</sup> an upper bound on outage probability is given by  $P_{outage} \leq 1 - \max\left(0, \sum_{k=1}^K \Pr(E_k > E_{th}) - K + 1\right) = \min\left(1, K - \sum_{k=1}^K \Pr(E_k > E_{th})\right)$ . Also,  $\Pr(E_k > E_{th}) = 1 - \Pr(E_k \leq E_{th})$ . And remaining proof steps to evaluate  $\Pr(E_k \leq E_{th})$  is given in detail in Appendix A. ■

<sup>5</sup>Let  $\Pr\left(\bigcap_{i=1}^r Q_i\right)$  be the joint probability of the events  $Q_1, \dots, Q_r$ , then according to Boole-Fréchet inequality [36],  $\max(0, \Pr(Q_1) + \dots + \Pr(Q_r) - (r-1)) \leq \Pr\left(\bigcap_{i=1}^r Q_i\right)$ .

#### IV. ANALYSIS OF PROBABILITY OF OUTAGE IN WET WITH ESTIMATED CSI

In this section, we first present estimation of the direct and the reflected channels via the IRS using the two step procedure described in Section III-A. Then we present our joint AS and IRS passive beamforming rule based on estimated CSI and derive its outage probability.

##### A. UL Pilot Transmission and Channel Estimation

*Step 1:* First, we estimate the direct path channel gain from  $S$  to  $U$ . In order to do that, we configure all the IRS elements to the off state, i.e.,  $\alpha_n = 0$  for all  $n = 1, \dots, N$ . The user transmits pilot  $x_p$  with power  $q$ . Then the source receives signal  $y^m$  when it connects RF chain to the  $m^{\text{th}}$  antenna. It is given by

$$y^m = \sqrt{q}h_{su}^m x_p + w^m, \quad \text{for } m = 1, \dots, M, \quad (18)$$

where  $|x_p|^2 = 1$  and  $w^m$  is the complex AWGN with zero mean and variance  $\sigma^2$ . We know that  $\bar{y}^m = y^m x_p^* = \sqrt{q}h_{su}^m + \bar{w}^m$ , where  $\bar{w}^m = w^m x_p^*$  is a sufficient statistic to estimate  $h_{su}^m$ . Based on  $\bar{y}^m$ , the MMSE estimate of the direct path channel gain is given by  $\hat{h}_{su}^m = \frac{\sqrt{q}\beta_{su}}{q\beta_{su} + \sigma^2} \bar{y}^m$  [37]. Substituting  $\bar{y}^m$ , it can be further simplified as

$$\hat{h}_{su}^m = h_{su}^m + \tilde{h}_{su}^m, \quad \text{for } m = 1, \dots, M, \quad (19)$$

where the channel estimation error  $\tilde{h}_{su}^m = \frac{-\sigma^2}{q\beta_{su} + \sigma^2} h_{su}^m + \frac{\sqrt{q}\beta_{su}}{q\beta_{su} + \sigma^2} \bar{w}^m$ . Note that  $\tilde{h}_{su}^m$  is independent of  $\hat{h}_{su}^m$ . Let  $\gamma_{su} = \mathbb{E} \left( \left| \hat{h}_{su}^m \right|^2 \right) = \frac{q\beta_{su}^2}{q\beta_{su} + \sigma^2}$  denote the variance of the channel estimate. Furthermore, the variance of the channel estimation error  $\mathbb{E} \left( \left| \tilde{h}_{su}^m \right|^2 \right) = \beta_{su} - \gamma_{su}$ . Let  $\hat{\rho}_{su}^m$  and  $\hat{\Lambda}_{su}^m$  respectively denote the magnitude and phase of the channel gain estimate  $\hat{h}_{su}^m$ , i.e.,  $\hat{h}_{su}^m = \hat{\rho}_{su}^m e^{j\hat{\Lambda}_{su}^m}$ , for  $m \in \{1, 2, \dots, M\}$ . The source selects antenna  $\hat{a}$  that has the highest channel power gain estimate. It is given by  $\hat{a} = \arg \max_{m \in \{1, 2, \dots, M\}} \{\hat{\rho}_{su}^m\}$ .

*Step 2:* The source connects the RF chain to antenna  $\hat{a}$  and estimates the corresponding cascaded channel gain via IRS. We turn on one IRS element at a time. The signal received at  $S$  when the  $n^{\text{th}}$  IRS element is turned on, i.e.,  $\alpha_n = 1$  and  $\theta_n = 0$ , is given by

$$y^{\hat{a}n} = \sqrt{q}h_{su}^{\hat{a}n} x_p + \sqrt{q}g_{siu}^{\hat{a}n} x_p + w^{\hat{a}n}, \quad \text{for } n = 1, \dots, N, \quad (20)$$

where  $w^{\hat{a}n}$  is complex AWGN with zero mean and variance  $\sigma^2$ . Let  $\bar{y}^{\hat{a}n} = y^{\hat{a}n} - \sqrt{q}h_{su}^{\hat{a}n} x_p$  denote the signal component after subtracting the scaled version of the direct path channel gain estimate obtained in Step 1. Using (19), we get  $\bar{y}^{\hat{a}n} = \sqrt{q}g_{siu}^{\hat{a}n} x_p + w^{\hat{a}n} - \sqrt{q}\tilde{h}_{su}^{\hat{a}n} x_p$ , for  $n = 1, \dots, N$ . A sufficient statistic to estimate the cascaded channel  $g_{siu}^{\hat{a}n}$  via the  $n^{\text{th}}$  IRS element is given by

$$\bar{\bar{y}}^{\hat{a}n} = \bar{y}^{\hat{a}n} x_p^* = \sqrt{q}g_{siu}^{\hat{a}n} + \bar{w}^{\hat{a}n} - \sqrt{q}\tilde{h}_{su}^{\hat{a}n}, \quad (21)$$

for  $n = 1, \dots, N$ , where  $\bar{w}^{\hat{a}n} = w^{\hat{a}n} x_p^*$ . Based on  $\bar{\bar{y}}^{\hat{a}n}$ , we next develop the linear MMSE estimate of the cascaded

channel coefficient between  $S$  and  $U$  via the  $n^{\text{th}}$  IRS element. Since, IRS is passive, estimate of the cascaded channel coefficients can only be obtained.

*Lemma 1:* The linear MMSE estimate of the cascaded channel coefficient  $g_{siu}^{\hat{a}n}$  between the selected antenna at  $S$  and  $U$  via the  $n^{\text{th}}$  IRS element is given by [37]

$$\hat{g}_{siu}^{\hat{a}n} = g_{siu}^{\hat{a}n} + \tilde{g}_{siu}^{\hat{a}n}, \quad (22)$$

where  $\tilde{g}_{siu}^{\hat{a}n}$  is given in (25),  $\mu_{si}^{\hat{a}n} = \sqrt{\frac{K_{si}\zeta_{si}}{K_{si}+1}} \bar{H}_{si}^{\hat{a}n}$ ,  $\mu_{iu}^n = \sqrt{\frac{K_{iu}\zeta_{iu}}{K_{iu}+1}} \bar{h}_{iu}^n$  and  $\mu_{siu}^{\hat{a}n} = \mu_{si}^{\hat{a}n} \mu_{iu}^n = \sqrt{\frac{K_{si}\zeta_{si}}{K_{si}+1} \frac{K_{iu}\zeta_{iu}}{K_{iu}+1}} \bar{H}_{si}^{\hat{a}n} \bar{h}_{iu}^n$ ,  $\tilde{\mu}_{su}^{\hat{a}n} = \mathbb{E} \left( \tilde{h}_{su}^{\hat{a}n} \right) = \Re \left( \tilde{\mu}_{su}^{\hat{a}n} \right) + j\Im \left( \tilde{\mu}_{su}^{\hat{a}n} \right)$ ,  $\Re \left( \tilde{\mu}_{su}^{\hat{a}n} \right) = \Im \left( \tilde{\mu}_{su}^{\hat{a}n} \right)$ ,  $\Re \left( \tilde{\mu}_{su}^{\hat{a}n} \right)$  and  $\left( \tilde{\sigma}_{su}^{\hat{a}n} \right)^2$  are given in (23) and (24), as shown at the bottom of the next page, respectively.

*Proof:* The proof is given in Appendix B. ■

##### B. DL Transmission Based on Estimated CSI

Let  $\hat{f}_i^n$  denote the reflection coefficient programmed at the  $n^{\text{th}}$  element based on the estimated CSI. Let  $\hat{h}_{su}^{\hat{a}} = \hat{\rho}_{su}^{\hat{a}} e^{j\hat{\Lambda}_{su}^{\hat{a}}}$  and  $\hat{g}_{siu}^{\hat{a}n} = \left| \hat{g}_{siu}^{\hat{a}n} \right| e^{j\hat{\phi}_{siu}^{\hat{a}n}}$  denote estimates of the direct and the reflected channels, respectively in terms of magnitude and phase. Substituting these estimates, in (7) and (8), joint AS and passive beamforming rule with estimated CSI can be written as

$$\hat{a} = \arg \max_{m \in \{1, 2, \dots, M\}} \{\hat{\rho}_{su}^m\}, \quad (26)$$

$$\hat{f}_i^n = \exp \left( -j \left( \hat{\phi}_{siu}^{\hat{a}n} - \hat{\Lambda}_{su}^{\hat{a}} \right) \right), \quad \text{for } n = 1, \dots, N. \quad (27)$$

Let  $\hat{\mathbf{f}}_i = \left[ \hat{f}_i^1, \hat{f}_i^2, \dots, \hat{f}_i^N \right]^T$  denote the IRS passive beamforming vector based on estimated CSI. Signal received at  $U$  when source employs above joint AS and passive beamforming rule is

$$\hat{y}_u = \left( h_{su}^{\hat{a}} + \mathbf{g}_{siu}^{\hat{a}} \hat{\mathbf{f}}_i \right) x_s + w_u, \quad (28)$$

where  $w_u \sim \mathcal{CN}(0, \sigma^2)$  denotes complex AWGN at the user. Here, we spend  $(M + N)\tau_p$  seconds to obtain channel estimates of the direct and reflected channel paths and energy is harvested for  $(\tau_c - (M + N)\tau_p)$  seconds in each coherence interval. Therefore, from (28), the harvested energy with estimated CSI is given by  $\hat{E}_u = \hat{\gamma} \left| h_{su}^{\hat{a}} + \mathbf{g}_{siu}^{\hat{a}} \hat{\mathbf{f}}_i \right|^2$ , where  $\hat{\gamma} = p\eta_r(\tau_c - (M + N)\tau_p)$ . Expressing true channel as sum of estimate and estimation error based on (19) and (22), we get

$$\hat{E}_u = \hat{\gamma} \left| \left( h_{su}^{\hat{a}} + \mathbf{g}_{siu}^{\hat{a}} \hat{\mathbf{f}}_i \right) - \left( \tilde{h}_{su}^{\hat{a}} + \tilde{\mathbf{g}}_{siu}^{\hat{a}} \hat{\mathbf{f}}_i \right) \right|^2. \quad (29)$$

Neglecting the estimation errors,  $\hat{E}_u$  in (29) can be approximated as

$$\begin{aligned} \hat{E}_u &\simeq \hat{\gamma} \left| h_{su}^{\hat{a}} + \mathbf{g}_{siu}^{\hat{a}} \hat{\mathbf{f}}_i \right|^2 \\ &= \hat{\gamma} \left| h_{su}^{\hat{a}} + \sum_{n=1}^N \hat{g}_{siu}^{\hat{a}n} \hat{f}_i^n \right|^2 \\ &= \hat{\gamma} \left| \hat{\rho}_{su}^{\hat{a}} e^{j\hat{\Lambda}_{su}^{\hat{a}}} + \sum_{n=1}^N \left| \hat{g}_{siu}^{\hat{a}n} \right| e^{j\hat{\phi}_{siu}^{\hat{a}n}} \hat{f}_i^n \right|^2. \end{aligned} \quad (30)$$

By triangle inequality, we know that the choice of  $\hat{f}_i^n$  in (27) maximizes  $\hat{E}_u$  in (30). Therefore, substituting  $\hat{f}_i^n$  from (27) in (30), the harvested energy can be written as

$$\hat{E}_u \simeq \hat{\gamma} \left( \hat{\rho}_{su} + \sum_{n=1}^N |\hat{g}_{siu}^{\hat{a}n}| \right)^2. \quad (31)$$

This approximation ensure analytical tractability. Furthermore, it is justified at practical operating points, since estimation errors  $\tilde{h}_{su}^{\hat{a}}$  and  $\tilde{g}_{siu}^{\hat{a}}$  make negligibly small contribution to  $\hat{E}_u$  [3], [38]. In Section V, our numerical results show that the probability of outage obtained through Monte Carlo simulations based on exact  $\hat{E}_u$  in (29) is in close agreement with the probability of outage expression derived in Theorem 3 based on approximate  $\hat{E}_u$  in (31).

### C. Analysis of Probability of Outage in WET

With estimated CSI, the probability of outage in WET is given by

$$\begin{aligned} \hat{P}_{\text{outage}} &= \Pr(\hat{E}_u \leq E_{\text{th}}) \\ &\simeq \Pr\left(\hat{\gamma} \left( \hat{\rho}_{su} + \sum_{n=1}^N |\hat{g}_{siu}^{\hat{a}n}| \right)^2 \leq E_{\text{th}}\right). \end{aligned} \quad (32)$$

Note that  $|\hat{g}_{siu}^{\hat{a}n}|$  is magnitude of the estimate of the cascaded channel coefficient from the selected antenna at  $S$  to  $U$  via  $n^{\text{th}}$  IRS element. To simplify the analysis, we model it as a Rician RV. Figure 2 plots the cumulative distribution function (CDF) of  $|\hat{g}_{siu}^{\hat{a}n}|$  obtained empirically from  $10^5$  samples through Monte Carlo simulations and the CDF of a Rician RV for three values of  $K_{si}$  and  $K_{iu}$ . We observe that for moderate and higher values of  $K_{si}$  and  $K_{iu}$ , the empirical and the Rician CDF match well. And for lower values of  $K_{si}$  and  $K_{iu}$ , we notice that the Rician approximation, while not perfect, tracks the empirical CDF of  $|\hat{g}_{siu}^{\hat{a}n}|$  reasonably well. For this model, we next derive mathematical expression that approximates  $\hat{P}_{\text{outage}}$  under estimated CSI.

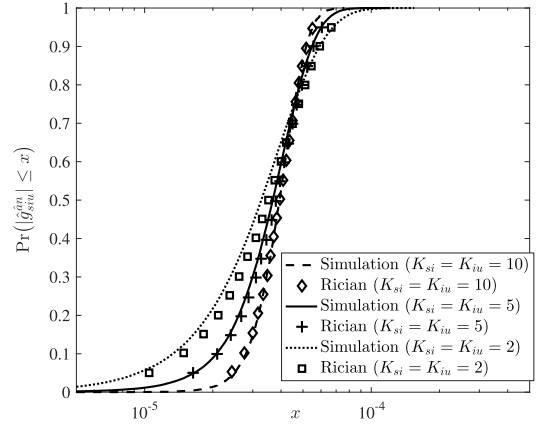


Fig. 2. CDF of  $|\hat{g}_{siu}^{\hat{a}n}|$  compared with Rician model with similar parameters ( $\beta_{su} = -45.81$  dB,  $\zeta_{si} = -46.67$  dB,  $\zeta_{iu} = -40.81$  dB,  $\sigma^2 = -100$  dBm, and  $q = 0$  dBm).

**Theorem 3:** With joint AS and IRS assisted passive beamforming based on estimated CSI, the probability of outage in WET is given by

$$\begin{aligned} \hat{P}_{\text{outage}} &\simeq \sum_{m=0}^{M-1} \frac{M(-1)^m}{m+1} \binom{M-1}{m} \left[ 1 - \hat{\psi} Q\left(\frac{\hat{E}_{\text{th}} - \mu_{\hat{y}}}{\sigma_{\hat{y}}}\right) \right. \\ &\quad \left. - \frac{\hat{\psi} e^{\frac{\hat{\xi}^2 - \hat{\eta} \hat{\chi}}{2\hat{\eta}}}}{\sqrt{\hat{\eta} \sigma_{\hat{y}}^2}} \left( Q\left(\frac{-\hat{\xi}}{\sqrt{\hat{\eta}}}\right) - Q\left(\frac{\hat{E}_{\text{th}} - \mu_{\hat{y}}}{\sigma_{\hat{y}} \sqrt{\hat{\eta}}}\right) \right) \right], \end{aligned} \quad (33)$$

where  $\hat{\psi} = Q^{-1}\left(\frac{-\mu_{\hat{y}}}{\sigma_{\hat{y}}}\right)$ ,  $\hat{\eta} = \frac{2(m+1)}{\gamma_{su}} + \frac{1}{\sigma_{\hat{y}}^2}$ ,  $\hat{\xi} = \frac{2(m+1)\hat{E}_{\text{th}}}{\gamma_{su}} + \frac{\mu_{\hat{y}}}{\sigma_{\hat{y}}}$ ,  $\hat{\chi} = \frac{2(m+1)\hat{E}_{\text{th}}^2}{\gamma_{su}} + \frac{\mu_{\hat{y}}^2}{\sigma_{\hat{y}}^2}$ ,  $\hat{E}_{\text{th}} = \sqrt{\frac{E_{\text{th}}}{\hat{\gamma}}}$ ,  $\mu_{\hat{y}} = N \sqrt{\frac{c_1^2 \pi}{4c_2}} L_{\frac{1}{2}}\left(\frac{-|\mu_{siu}^{\hat{a}n}|^2 c_2}{c_1^2}\right)$ ,  $\sigma_{\hat{y}}^2 = N \left(\frac{c_1^2}{c_2} + |\mu_{siu}^{\hat{a}n}|^2 - \hat{\mu}_0^2\right)$ ,  $\hat{\mu}_0 = \sqrt{\frac{c_1^2 \pi}{4c_2}} L_{\frac{1}{2}}\left(\frac{-|\mu_{siu}^{\hat{a}n}|^2 c_2}{c_1^2}\right)$ ,  $c_1 = \sqrt{q} \left( (\beta_{si} + |\mu_{si}^{\hat{a}n}|^2) (\beta_{iu} + |\mu_{iu}^n|^2) - |\mu_{siu}^{\hat{a}n}|^2 \right)$ , and  $c_2 = q \left( \beta_{si} + |\mu_{si}^{\hat{a}n}|^2 \right) (\beta_{iu} + |\mu_{iu}^n|^2) + \sigma^2 - q |\mu_{siu}^{\hat{a}n}|^2$ .

*Proof:* The proof is given in Appendix C. ■

$$\Re(\tilde{\mu}_{su}^{\hat{a}}) \simeq \frac{-M\sqrt{\beta_{su} - \gamma_{su}}}{2\sqrt{\pi}} \left( \sum_{m=0}^{M-1} \binom{M-1}{m} \left(\frac{-1}{12}\right)^{M-1} 3^{m+1} - \sum_{m_1=0}^{M-1} \sum_{m_2=0}^{m_1} \binom{M-1}{m_1} \binom{m_1}{m_2} \left(\frac{-1}{12}\right)^{m_1} 3^{m_2+1} \right), \quad (23)$$

$$\begin{aligned} (\tilde{\sigma}_{su}^{\hat{a}})^2 &= \text{var}(\tilde{h}_{su}^{\hat{a}}) \simeq \frac{M(\beta_{su} - \gamma_{su})}{2} \left( \sum_{m_1=0}^{M-1} \sum_{m_2=0}^{m_1} \binom{M-1}{m_1} \binom{m_1}{m_2} \left(\frac{-1}{12}\right)^{m_1} 3^{m_2+1} \frac{\sqrt{3(3m_1 + m_2 + 3)}}{(3m_1 + m_2 + 3)^2} \right. \\ &\quad \left. + \sum_{m=0}^{M-1} \binom{M-1}{m} \left(\frac{1}{12}\right)^{M-1} 3^{m+1} \frac{\sqrt{3(3M + m)}}{(3M + m)^2} \right) - |\tilde{\mu}_{su}^{\hat{a}}|^2. \end{aligned} \quad (24)$$

$$\begin{aligned} \tilde{g}_{siu}^{\hat{a}n} &= \frac{-g_{siu}^{\hat{a}n} [\sigma^2 + q(\tilde{\sigma}_{su}^{\hat{a}})^2]}{q(\beta_{si} + |\mu_{si}^{\hat{a}n}|^2)(\beta_{iu} + |\mu_{iu}^n|^2) + \sigma^2 + q(\tilde{\sigma}_{su}^{\hat{a}})^2 - q|\mu_{siu}^{\hat{a}n}|^2} + \mu_{siu}^{\hat{a}n} \\ &\quad + \frac{\sqrt{q} \left( (\beta_{si} + |\mu_{si}^{\hat{a}n}|^2) (\beta_{iu} + |\mu_{iu}^n|^2) - |\mu_{siu}^{\hat{a}n}|^2 \right) \left[ \tilde{w}^{\hat{a}n} - \sqrt{q} \tilde{h}_{su}^{\hat{a}} - \sqrt{q} (\mu_{siu}^{\hat{a}n} - \tilde{\mu}_{su}^{\hat{a}}) \right]}{q(\beta_{si} + |\mu_{si}^{\hat{a}n}|^2)(\beta_{iu} + |\mu_{iu}^n|^2) + \sigma^2 + q(\tilde{\sigma}_{su}^{\hat{a}})^2 - q|\mu_{siu}^{\hat{a}n}|^2}. \end{aligned} \quad (25)$$

The analysis above accounts for order statistics of the magnitude of the estimated channel coefficients along the direct path and design of phase-shifts at  $I$  based on CSI estimates. Unlike the  $P_{\text{outage}}$  expression for perfect CSI in (11),  $\hat{P}_{\text{outage}}$  in (33) is a function of the pilot power  $q$ , the time  $(\tau_c - (M + N)\tau_p)$  that is used for DL WET, noise power  $\sigma^2$  that accounts for estimation errors, and the statistics of the estimated CSI. Furthermore, the expression in (33) also brings out the dependence of  $\hat{P}_{\text{outage}}$  on system and channel parameters. At high pilot power,  $\hat{P}_{\text{outage}}$  in (33) reduces to  $P_{\text{outage}}$  in (11), since  $\mu_{\hat{y}} \rightarrow \mu_y$ ,  $\sigma_{\hat{y}}^2 \rightarrow \sigma_y^2$  and  $\gamma_{su} \rightarrow \beta_{su}$ .

1) *Diversity Order*: We refer to the slope of the probability of outage versus the source transmit power curve in the asymptotic regime in a log-log scale as the diversity order in WET systems. We now derive the diversity order with estimated CSI in terms of number of antennas at the source and the number of passive reflecting elements at the IRS.

*Theorem 4*: The diversity order of a joint AS and IRS passive beamforming assisted WET system with estimated CSI is  $M + N$ .<sup>6</sup>

*Proof*: The proof is given in Appendix D. ■

2) *Extension to Multi-User Scenario*: With estimated CSI,  $K(M + N)\tau_p$  seconds in a coherence interval would be spent on pilots. And AS at source and passive beamforming at IRS will be performed with estimated CSI. Therefore, based on round-robin scheduling strategy, the source would transfer energy wirelessly to every user over a slot of length  $\frac{(\tau_c - K(M + N)\tau_p)}{K}$ .

*Theorem 5*: An upper bound on probability of outage in WET with estimated CSI when users are served based on round-robin scheduling strategy is given by

$$\hat{P}_{\text{outage}} \leq \min \left( 1, \sum_{k=1}^K \Pr \left( \hat{E}_k \leq E_{\text{th}} \right) \right), \quad (34)$$

where  $\hat{E}_k$  denotes the energy harvested by the  $k^{\text{th}}$  user with estimated CSI and  $\Pr \left( \hat{E}_k \leq E_{\text{th}} \right)$  is given in Theorem 3 with  $\hat{\gamma} = \frac{p\eta_r(\tau_c - K(M + N)\tau_p)}{K}$ .

This can be proved along similar lines using ideas from Theorem 2 and Appendix C.

## V. NUMERICAL RESULTS

In this section, we present numerical results to illustrate the potential of joint low complexity AS at source and passive beamforming at IRS for WET. We present results to show the impact of the system parameters such as number of antennas  $M$  at source, number of IRS elements  $N$ , source transmit power  $p$  and pilot power  $q$  on the probability of outage. Unless mentioned otherwise, for illustration, we take  $E_{\text{th}} = 10^{-7}$  J,  $p = 1$  W,  $q = 1$  mW,  $\tau_c = 10$  ms,  $\eta_r = 0.5$ ,  $\tau_p = \frac{0.01\tau_c}{M + N}$ ,  $\sigma^2 = 10^{-13}$  W,  $K = 1$ ,  $K_{si} = 10$ ,  $K_{iu} = 10$ ,  $\zeta_{ab} = \frac{G_a G_b \varpi}{d_{ab}^\rho}$ , where  $a, b \in \{s, u, i\}$ ,  $\varpi = \left(\frac{d}{2\pi}\right)^2$  is the average channel

<sup>6</sup>Note that this result is valid when the wireless channel offers rich scattering. It can therefore be considered as the maximal diversity gain that one can extract from such a system.

attenuation at unit reference distance with  $d = \frac{c}{2f}$  denoting the inter-element separation at the IRS,  $f = 915$  MHz,  $c = 3 \times 10^8$  m/s denotes speed of light and  $d_{ab}$  denotes distance between  $a$  and  $b$ . Furthermore, we take  $G_s = G_u = 0$  dBi,  $G_i = 5$  dBi and the path loss exponent  $\rho = 2$  [5]. We consider that  $S$ ,  $I$ , and  $U$  are arranged in a rectangular topology,  $S$  and  $I$  are placed opposite to each other with their coordinates (in meters) as  $(0, 0)$  and  $(10, 0)$  respectively, and  $U$  is placed at  $(5, 1)$ .

Figure 3 (a) plots probability of outage in WET as a function of  $N$  for three configurations, namely,  $C = (1, 1)$ ,  $C = (1, 2)$  and  $C = (1, 4)$  and for both perfect and estimated CSI. Note that  $C = (N_{\text{RF}}, M)$  refers to the configuration where the source is equipped with  $N_{\text{RF}}$  RF chains and  $M$  antennas. We note that the Monte Carlo simulations are in close agreement with analysis for both perfect and estimated CSI thus validating our analysis. We observe that with  $N = 70$ , the probability of outage when  $C = (1, 4)$  is lower by factors 100x and 1000x when compared to  $P_{\text{outage}}$  with  $C = (1, 2)$  and  $C = (1, 1)$ , respectively. This is because the diversity order increases as  $M$  increases. We also observe that outage probability degrades marginally with estimated CSI due to estimation errors and the fact that a part of the coherence interval is spent in estimation.

Figure 3 (b) plots probability of outage as a function of  $p$  for  $C = (1, 1)$  and  $C = (1, 4)$  and for two values of  $N$ . This is again done for both perfect and estimated CSI. As before, analysis matches well with simulations. We observe that the required transmit power at the source to achieve a given probability of outage decreases as the number of IRS elements increases. For example, with  $C = (1, 4)$ , we can achieve  $P_{\text{outage}}$  of  $10^{-6}$  with 5 dBW lower transmit power at  $S$  by adding 100 extra IRS elements. Moreover, the diversity order, which is equal to  $M + N$ , increases as  $M$  or  $N$  increase.

Figure 4 (a) plots probability of outage as a function of  $q$  for both perfect and estimated CSI. In general, the threshold energy  $E_{\text{th}}$  required at the user depends on the energy  $E_p$  spent on performing assigned tasks and the energy spent on channel estimation, i.e.,  $q(M + N)\tau_p$ . To illustrate the impact of  $q$ , we consider  $E_p = 10^{-7}$  J and  $E_{\text{th}} = E_p + q(M + N)\tau_p$ . With estimated CSI, we observe three regions of operation: i) For small values of pilot power, the probability of outage is high due to high channel estimation errors, ii) For medium values of pilot powers, i.e.,  $-70$  dBW  $\leq q \leq -40$  dBW with  $N = 75$ , the probability of outage is relatively insensitive to the increase in pilot power, iii) For large values of pilot power, i.e.,  $q \geq -40$  dBW with  $N = 75$ , large amount of energy is spent for channel estimation. This increases  $E_{\text{th}}$ , which in turn, increases the probability of outage. Under perfect CSI, the outage probability is constant for smaller values of  $q$ . This is because  $q(M + N)\tau_p \ll E_p$  and  $P_{\text{outage}}$  does not depend on estimation errors. Furthermore,  $P_{\text{outage}}$  increases as  $q$  increases beyond  $-40$  dBW since the threshold increases.<sup>7</sup>

<sup>7</sup>We show the outage performance with perfect CSI as well to elucidate and quantify the loss in outage performance due to estimation errors. The threshold energy under perfect CSI is kept the same as that with estimated CSI to ensure fair comparison.

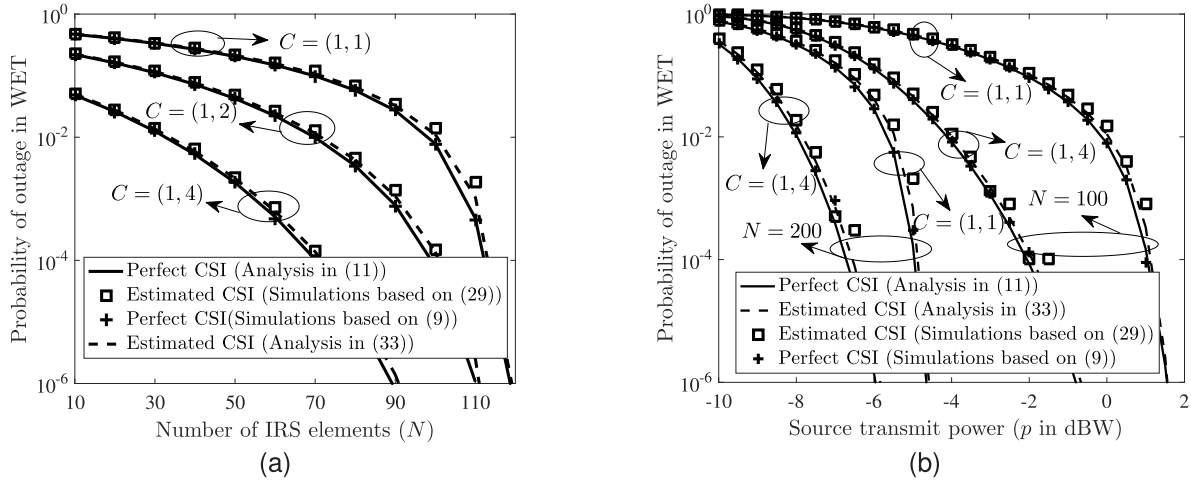


Fig. 3. (a) Impact of  $N$  ( $p = 1$  W,  $q = 1$  mW,  $K = 1$ , and  $E_{th} = 10^{-7}$  J). (b) Impact of  $p$  ( $q = 1$  mW,  $K = 1$ , and  $E_{th} = 10^{-7}$  J).

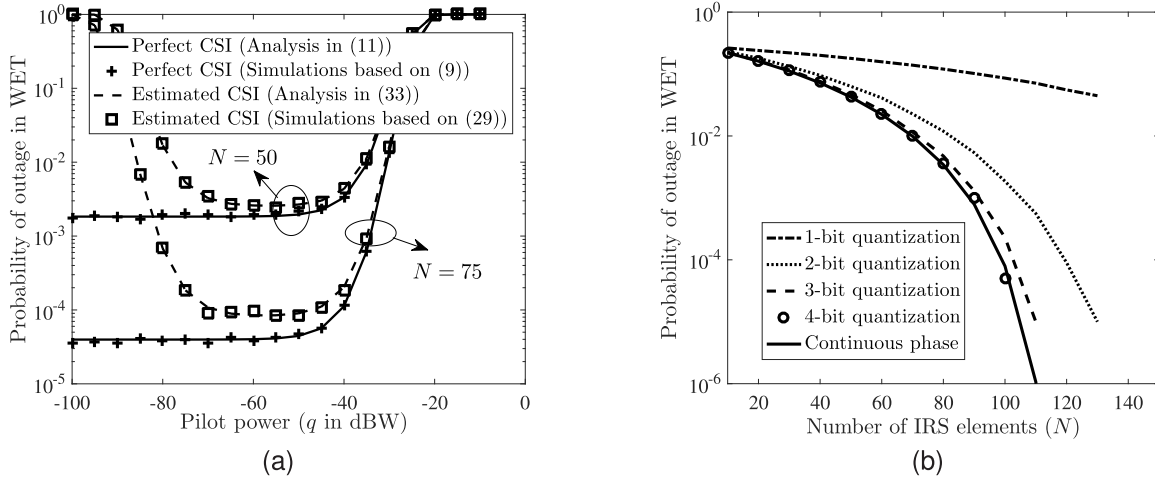


Fig. 4. (a) Impact of  $q$  ( $p = 1$  W,  $E_{th} = E_p + q(M + N)\tau_p$ ,  $C = (1, 4)$ ,  $K = 1$ , and  $E_p = 10^{-7}$  J), (b) Impact of discrete phase shifts ( $p = 1$  W,  $C = (1, 2)$ ,  $K = 1$ , and  $E_{th} = 10^{-7}$  J).

**Discrete Phase Shifts:** Figure 4 (b) plots probability of outage in WET as a function of  $N$  under both continuous and discrete phase shifts at the IRS. We obtain the discrete phase shift by quantizing the continuous phase shift to the nearest available quantization level. We note that with  $j$ -bit discrete phase shifter at the IRS,  $2^j$  phase-shift quantization levels are possible. As the number of quantization bits used to program the IRS increases, the performance with discrete phase shifts gets closer to the performance with continuous phase shifts. This is because an increase in the resolution of the discrete phase shifts enables better coherent combination of the reflected and direct path signals. In fact, a 3-bit programmable IRS is sufficient to achieve good trade-off between complexity<sup>8</sup> and performance.

Figure 5 (a) plots probability of outage in WET vs.  $N$  for  $K = 2$  and 4 with perfect and estimated CSI. Analysis matches

<sup>8</sup>To configure phase shifts, positive-intrinsic-negative (PIN) diodes are used in the control circuitry at the IRS. With one PIN diode in the control circuitry at the IRS, only phase shifts of 0 and  $\pi$  can be induced. To induce an  $Q$ -level phase shift per IRS element,  $\log_2(Q)$  PIN diodes would be required.

well with simulations, thus confirming the tightness of the upper bound. We observe that by increasing  $N$ , WET to a larger number of users can be supported while maintaining the outage probability fixed at a specific level. For example, 100 extra IRS elements are required to support WET to 4 users when compared against WET to 2 users while maintaining outage probability fixed at  $10^{-4}$ .

**Performance Benchmarking:** We benchmark the performance of the proposed AS rule with the selection rules considered in the literature.

1) **Optimal Antenna Selection (OAS) rule** [17], [18]: With estimated CSI, the OAS rule is given by  $\hat{a}^{OAS} = \arg \max_{1 \leq m \leq M} \left( \left| \hat{h}_{su}^m \right| + \sum_{n=1}^N \left| \hat{g}_{snu}^{mn} \right| \right)$ . This rule maximizes the receive power under perfect CSI. However, it requires  $M + MN$  pilot transmissions to obtain CSI. This is much higher than the  $M + N$  pilot transmissions required by our proposed AS rule.

2) **Low Complexity Antenna Selection (LAS) rule** [17]: With estimated CSI, the LAS rule is given by  $\hat{a}^{LAS} =$

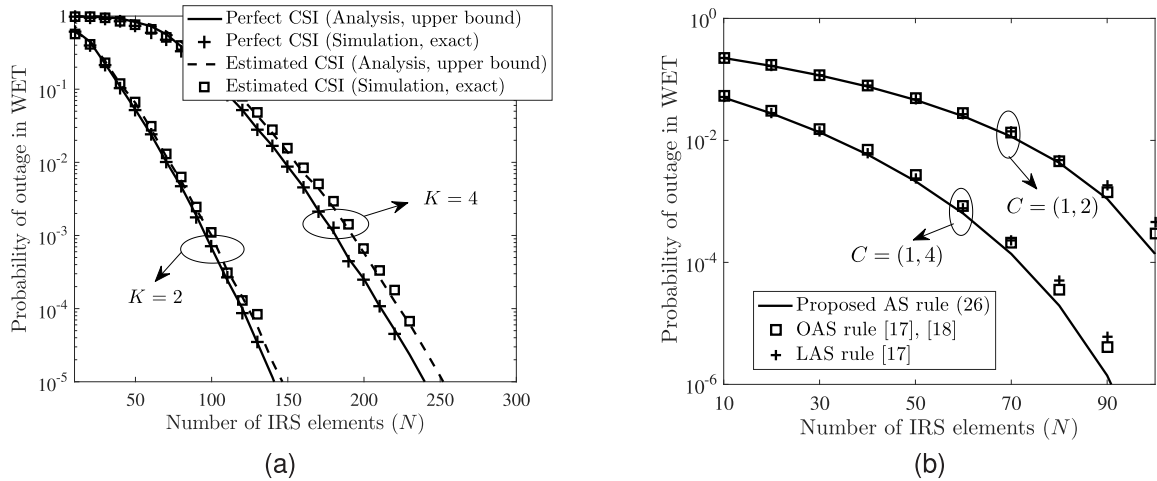


Fig. 5. (a) Impact of number of users ( $p = 1$  W,  $q = 1$  mW,  $C = (1, 4)$  and  $E_{th} = 10^{-7}$  J). Users are distributed uniformly between  $(0, 1)$  and  $(10, 1)$ , (b) Performance benchmarking: Impact of different AS strategies ( $p = 1$  W,  $q = 1$  mW,  $K = 1$ , and  $E_{th} = 10^{-7}$  J).

$\arg \max_{1 \leq m \leq M} \left( |h_{su}^m| + \left| \sum_{n=1}^N g_{snu}^{mn} \right| \right)$ . It requires  $2M + N$  pilots transmission to obtain the CSI. Both OAS and LAS rules configure IRS elements as in (27).

Figure 5 (b) compares the performance of the proposed AS rule with the above two AS rules. It plots the probability of outage vs.  $N$  with estimated CSI for two different configurations. For  $C = (1, 2)$ , we see that the proposed AS rule<sup>9</sup> performs very close to OAS and LAS rules, which consider reflected channel gains in addition to the direct path channel gains. This is because the strength of the reflected channel gain via the IRS is relatively weaker compared to the strength of the direct path channel gain. We note that the proposed AS rule performs close to the optimal rule while requiring fewer number of pilot transmissions. For  $C = (1, 4)$ , as  $N$  increases, we see that the proposed AS rule performs better than the OAS and LAS rules. This is due to increase in the time required for the pilot transmission for both OAS and LAS rules, which in turn reduces the time available for DL energy transmission. For OAS and LAS rules, the time available for DL energy transfer is  $(\tau_c - (M + MN)\tau_p)$  and  $(\tau_c - (2M + N)\tau_p)$  seconds, respectively, while the proposed AS rule has  $(\tau_c - (M + N)\tau_p)$  seconds available for energy transfer. Furthermore, the OAS rule performs marginally better than the LAS rule despite having a smaller DL energy transmission duration since it by design maximizes the receive power under perfect CSI.

**Subset AS:** Figure 6 (a) plots the PTE<sup>10</sup> as a function of the number of RF chains at the source for  $M = 32$  and

<sup>9</sup>Unlike information transfer, in which the range is of the order of hundreds of meters, the range of WET is very limited and typically varies from few meters to few tens of meters [3]–[5]. In most WET scenarios, it is, therefore, more likely that the direct channel between the source and the user would be present. And in WET, it is the absolute receive power that matters, unlike information transfer where the receive signal-to-noise ratio is of interest. And by using IRS-assisted beamforming, the receive power can be boosted significantly to compensate the loss in performance due to AS.

<sup>10</sup>It is defined as the ratio of the average power harvested by the user to the total average power consumed at the source. Please note we model the total average power consumed at the source as  $P_c = p_{tx} + p_{fix} + N_{RF}p_s + p_{ip} + Np_e$  [38], [39], where  $p_{tx} = \frac{p}{\eta_{pa}}$ ,  $p$  denotes the source transmit power,  $\eta_{pa}$  denotes the efficiency of the power amplifier at the source,  $p_{fix}$  denotes the fixed power required to run the source,  $p_s$  denotes the circuit power consumed in every RF chain at the source,  $N_{RF}$  denotes the number of RF chains,  $p_{ip} =$

$N = 50, 75, \text{ and } 100$ . We observe that the PTE increases initially as the number of RF chains increase and reaches a maxima. This is because the power harvested by the user increases as more number of antennas are selected<sup>11</sup> for energy beamforming. However, beyond a certain number of RF chains, the PTE decreases as the power consumption at the source dominates the harvested power at the user. Therefore, employing subset AS with a certain number of RF chains yields optimal PTE when compared to employing full complexity energy beamforming where number of RF chains must equal the number of antennas. For a given number of RF chains at the source, the PTE improves as  $N$  increases.

Figure 6 (b) plots the probability of outage as a function of  $p$  for  $N = 50$  and  $N = 150$  and for different configurations. We observe that for a given source transmit power, the outage probability of single AS (1, 4) with  $N = 150$  is lower than even a full complexity (4, 4) system with  $N = 50$ . Thus, one can trade-off active RF chains at the source with passive elements at the IRS to obtain improved outage performance. We also note that for a given configuration, substantial savings of radiated power is obtained by adding few passive elements at the IRS while maintaining the same outage probability.

**Limited Scattering:** To study the impact of limited scattering on the probability of outage in WET, we model and decompose the channels as in [23]. Based on this physics based generic model [14], [23], the  $n^{\text{th}}$  entry of the phase shift matrix is given by  $[\Theta]_{nn} = \alpha_n e^{j\theta_n}$ , where  $\alpha_n^2 = \left( \frac{\sqrt{4\pi}}{\lambda} |g_i(\Phi_t, \Phi_r)| \right)^2$ , for all  $n$ , captures the amount by which the product of the path losses from source to IRS and IRS to user would get affected due to the ampli-

$\frac{3N_{RF}KB}{S_c k_s}$  denotes the total power consumed in computing active beamformer at the source,  $B$  denotes the system bandwidth,  $S_c = B_c \tau_c$  denotes the number of samples in a coherence block,  $B_c$  denotes the coherence bandwidth,  $\tau_c$  denotes the length of the coherence interval,  $K$  denotes the number of users,  $k_s$  denotes the source computational efficiency (in flops/watt) and  $p_e$  denotes the power spent in configuring the phase shift at each IRS element.

<sup>11</sup>For subset AS, the direct link channel power gains are arranged in descending order and  $N_{RF}$  antennas with the highest channel gains are selected. The active beamformer at the source and the phase-shifts at the IRS for both subset AS and the full-complexity system are obtained to maximize the received power based on alternating optimization [25].

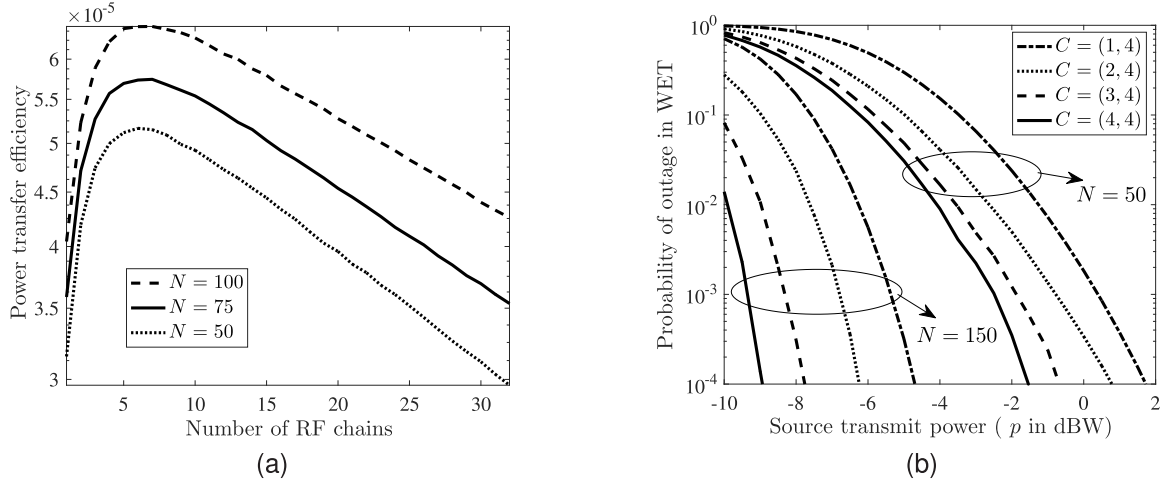


Fig. 6. Illustration of trade-off between RF chains at source and passive elements at IRS (a) PTE vs. number of RF chains ( $M = 32$ ,  $p = 1$  W,  $p_s = 1$  W,  $p_{\text{fix}} = 1$  W,  $\eta_{\text{pa}} = 0.39$ ,  $p_e = 5$  mW,  $K = 1$ ,  $B = 10$  MHz,  $B_c = 10$  KHz, and  $k_s = 20 \times 10^9$  flops/W). (b)  $P_{\text{outage}}$  vs.  $p$  ( $K = 1$  and  $E_{\text{th}} = 10^{-7}$  J).

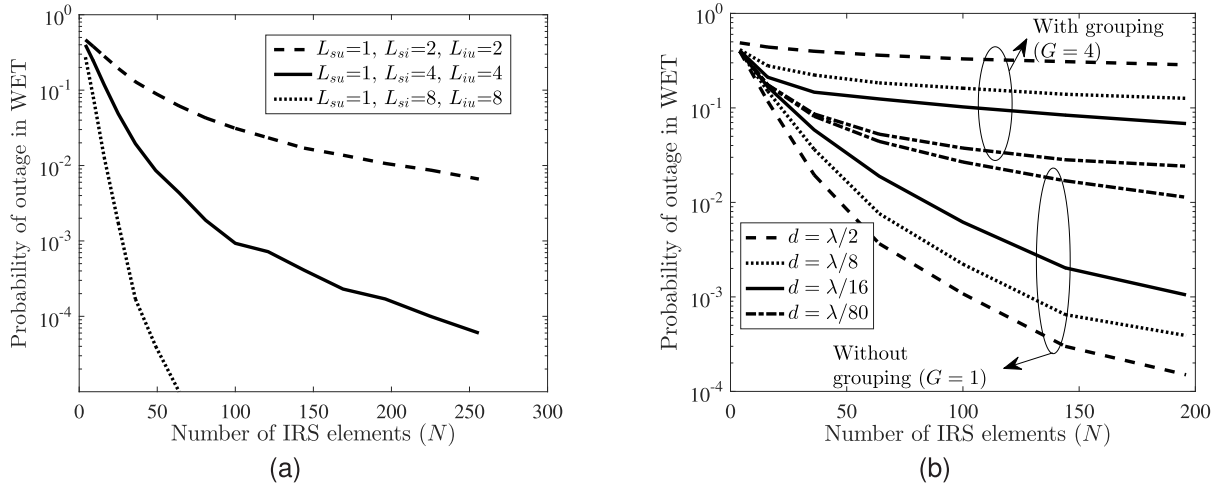


Fig. 7. (a) Impact of limited scattering ( $p = 1$  W,  $K = 1$ ,  $\tau' = 0.8$ ,  $C = (1, 4)$ ,  $E_{\text{th}} = 10^{-7}$  J, and  $l_i = d = \frac{\lambda}{2}$ ), (b) Impact of  $d$  ( $p = 1$  W,  $K = 1$ ,  $\tau' = 0.8$ ,  $E_{\text{th}} = 10^{-7}$  J,  $l_i = \frac{\lambda}{2}$ ,  $C = (1, 4)$ ,  $L_{su} = 1$ , and  $L_{si} = L_{iu} = 4$ ).

tude change induced by the IRS.<sup>12</sup> Note that  $g_i(\Phi_t, \Phi_r) = j \frac{\sqrt{4\pi}}{\lambda} \tau' l_i^2 \tilde{g}_i(\Phi_t, \Phi_r)$  denotes the response of each reflection element at IRS,  $\tau'$  denotes amplitude of the reflection coefficient,  $l_i^2$  captures the area of an IRS element,  $\Phi_t$  denotes the direction of the incident signal,  $\Phi_r$  denotes the direction of the reflected signal, and  $\tilde{g}_i(\Phi_t, \Phi_r)$  is given in [23, Eqn. (11)].

Figure 7 (a) plots probability of outage in WET as a function of  $N$  under limited scattering. Note that  $L_{su}$ ,  $L_{si}$ , and  $L_{iu}$  denote the number of scatterers in the channel from  $S$  to  $U$ ,  $S$  to  $I$ , and  $I$  to  $U$ , respectively. We observe that outage probability increases as number of scatterers in the channel reduce. This is because the channel becomes more and more spatially correlated as the number of scatterers decrease.

<sup>12</sup>For this model,  $\mu_0$  in Section III-B1 can be expressed in a generic form as  $\mu_0 = \frac{\pi}{4} \sqrt{\alpha_n^2 \beta_{si} \beta_{iu}} L_{\frac{1}{2}}(-K_{si}) L_{\frac{1}{2}}(-K_{iu})$ . Using this, (15) is modified as  $\frac{\lambda^2 \sqrt{E_{\text{th}}}}{\tau' l_i^2 \tilde{g}_i(\Phi_t, \Phi_r) \pi^2 \sqrt{p \eta_r \tau_c} \sqrt{\beta_{si} \beta_{iu}} L_{\frac{1}{2}}(-K_{si}) L_{\frac{1}{2}}(-K_{iu})}$ . This expression brings out dependence on the size  $l_i$  of each reflecting element at the IRS, and also gives insight that as size of IRS elements decreases, we need more IRS elements to avoid outage. The corresponding analysis under LoS scenario can be done along similar lines.

The channel correlation can be exploited to further reduce the number of pilot transmissions by considering grouping based channel estimation.<sup>13</sup> We configure the phase shift of any element in a group of size  $G$  as  $f_i^g = \exp(-j(\phi_{siu}^{aG} - \Lambda_{su}^a))$ , for all  $g \in \{1, \dots, G\}$ , where  $\phi_{siu}^{aG} = \angle H_{si}^{aG} + \angle h_{iu}^G$ ,  $\Lambda_{su}^a = \angle h_{su}^a$  and  $a$  denotes the strongest antenna along the direct path to the user. This grouping further reduces the pilot transmissions to  $M + \frac{N}{G}$  [41]. To illustrate performance with grouping under limited scattering, Figure 7 (b) plots outage probability vs.  $N$  for different inter-element spacing ( $d$ ) and for two values of  $G$ . We observe that the gap between outage probability with  $G = 1$  and  $G = 4$  decreases as  $d$  decreases. This is due to increase in spatial correlation as inter-element spacing decreases. Therefore, this underlying correlation can be exploited to configure a larger group of adjacent elements with identical phase-shifts.

<sup>13</sup>The authors in [40] exploit the sparse structure of the wireless channel at mmWave frequencies to reduce channel estimation overhead. However, we focus on WET at sub-6 GHz, where the channel is not really sparse.

## VI. CONCLUSION

We considered a WET system in which a source with multiple antennas and a single RF chain transfers energy to an energy-constrained user and is assisted by an IRS with passive reflecting elements. We proposed a joint AS and passive beamforming rule that selects antenna based on direct path channel gains. We showed that it is near-optimal with fewer pilot transmissions. We derived new mathematical expressions for probability of outage for both perfect and estimated CSI cases and for both single and multi-user scenarios. We also proved that the diversity order of joint AS and IRS beamforming assisted system equals sum of the number of antennas at the source and the number of passive reflecting elements at the IRS.

We showed that the source transmit power required to achieve a target outage probability decreases as the number of IRS elements or the number of transmit antennas increase. With estimated CSI, we observed that probability of outage is high both at low pilot powers due to high channel estimation errors and at high pilot powers as large fraction of the harvested energy is spent on channel estimation. We proved that we can trade-off active RF chains at source with passive elements at IRS to obtain improved performance both in terms of outage probability and PTE. We also showed that by adding few passive IRS elements, WET to a larger number of users can be supported. Furthermore, a 3 bit programmable IRS gives near-identical outage probability as a continuous phase shift IRS. We also elucidated the impact of limited scattering on performance. Outage analysis with multiple IRS is an interesting avenue for future work.

## APPENDIX

### A. Brief Proof of Theorem 1

We are interested in evaluating  $P_{\text{outage}} = \Pr\left(\gamma\left(\rho_{su}^a + \sum_{n=1}^N \rho_{siu}^{an}\right)^2 \leq E_{\text{th}}\right)$ . Let  $X = \rho_{su}^a = \max\{\rho_{su}^1, \dots, \rho_{su}^M\}$  and  $Y = \sum_{n=1}^N \rho_{siu}^{an} = \sum_{n=1}^N \rho_{si}^{an} \rho_{iu}^n$ . Thus,  $P_{\text{outage}}$  can be re-written as

$$P_{\text{outage}} = \int_{y=0}^{\infty} \Pr(X \leq \bar{E}_{\text{th}} - Y | Y = y) f_Y(y) dy$$

$$= \int_{y=0}^{\bar{E}_{\text{th}}} \int_{x=0}^{\bar{E}_{\text{th}} - y} f_X(x) f_Y(y) dx dy, \quad (35)$$

where  $\bar{E}_{\text{th}} = \sqrt{\frac{E_{\text{th}}}{\gamma}}$ ,  $f_X(x)$  is the pdf of  $X$ ,  $f_Y(y)$  is the pdf of  $Y$ . The equality in (35) holds since  $X$  and  $Y$  are mutually independent non-negative real RVs. To derive  $P_{\text{outage}}$  we need to compute  $f_X(x)$  and  $f_Y(y)$ . Since,  $X$  is the maximum of  $M$  i.i.d. Rayleigh RVs. Based on order statistics, it can be shown that  $f_X(x) = \frac{2Mx}{\beta_{su}} \left(1 - \exp\left(-\frac{x^2}{\beta_{su}}\right)\right)^{M-1} \exp\left(-\frac{x^2}{\beta_{su}}\right)$ ,  $x \geq$

0 [42]. To compute  $f_Y(y)$ , we invoke central limit theorem (CLT) [35]. Based on CLT, with large  $N$ , distribution of the sum of product of i.i.d. Rician RVs approaches Gaussian distribution and its pdf is given by  $f_Y(y) = \frac{\psi}{\sqrt{2\pi\sigma_y^2}} \exp\left(-\frac{(y-\mu_y)^2}{2\sigma_y^2}\right)$ ,  $y \geq 0$ , where the scaling constant  $\psi = Q^{-1}\left(\frac{-\mu_y}{\sigma_y}\right)$  ensures that  $\int_0^{\infty} f_Y(y) dy = 1$ . Based on the  $r^{\text{th}}$  moment of Rician RVs and exploiting the fact that  $\rho_{si}^{an}$  is independent of  $\rho_{iu}^n$ ,  $\mu_y$  and  $\sigma_y$  can be obtained as stated in Theorem 1.

Substituting the pdf of  $X$  in (35) and using binomial expansion to simplify,

$$P_{\text{outage}} = \int_{y=0}^{\bar{E}_{\text{th}}} \left( \int_{x=0}^{\bar{E}_{\text{th}} - y} \sum_{m=0}^{M-1} (-1)^m M \binom{M-1}{m} \frac{2x}{\beta_{su}} \times \exp\left(-\frac{x^2(m+1)}{\beta_{su}}\right) dx \right) f_Y(y) dy. \quad (36)$$

Solving the inner integral above with respect to  $x$ , we get

$$P_{\text{outage}} = \sum_{m=0}^{M-1} (-1)^m \frac{M}{m+1} \binom{M-1}{m} \left( \underbrace{\int_{y=0}^{\bar{E}_{\text{th}}} f_Y(y) dy}_{I_1} - \underbrace{\int_{y=0}^{\bar{E}_{\text{th}}} \exp\left(-\frac{(y-\bar{E}_{\text{th}})^2(m+1)}{\beta_{su}}\right) f_Y(y) dy}_{I_2} \right). \quad (37)$$

Substituting the pdf of  $Y$  from above and simplifying  $I_1$  and  $I_2$ , we obtain  $P_{\text{outage}}$  in (11).

### B. Proof of Lemma 1

Based on  $\bar{y}^{\hat{a}n}$ , the linear MMSE estimate of  $g_{siu}^{\hat{a}n}$  is given by [37]

$$\hat{g}_{siu}^{\hat{a}n} = \mathbb{E}(g_{siu}^{\hat{a}n}) + R_{g_{siu}^{\hat{a}n} \bar{y}^{\hat{a}n}} R_{\bar{y}^{\hat{a}n} \bar{y}^{\hat{a}n}}^{-1} \left[ \bar{y}^{\hat{a}n} - \mathbb{E}(\bar{y}^{\hat{a}n}) \right]. \quad (38)$$

It can be shown that  $\mathbb{E}(g_{siu}^{\hat{a}n}) = \mu_{siu}^{\hat{a}n}$  and  $\mathbb{E}(\bar{y}^{\hat{a}n}) = \sqrt{q}(\mu_{siu}^{\hat{a}n} - \tilde{\mu}_{su}^{\hat{a}n})$ , where  $\mu_{siu}^{\hat{a}n}$  and  $\tilde{\mu}_{su}^{\hat{a}n}$  are as stated in Lemma 1. Furthermore, the cross-correlation  $R_{g_{siu}^{\hat{a}n} \bar{y}^{\hat{a}n}}$  between the cascaded channel  $g_{siu}^{\hat{a}n}$  and the observable  $\bar{y}^{\hat{a}n}$  is given by

$$R_{g_{siu}^{\hat{a}n} \bar{y}^{\hat{a}n}} = \mathbb{E}(g_{siu}^{\hat{a}n} \bar{y}^{\hat{a}n*}) - \mu_{siu}^{\hat{a}n} \mathbb{E}(\bar{y}^{\hat{a}n})^*. \quad (39)$$

Substituting  $\bar{y}^{\hat{a}n}$  from (21) and  $\mathbb{E}(\bar{y}^{\hat{a}n})$  mentioned above, in (39), and simplifying, we get

$$R_{g_{siu}^{\hat{a}n} \bar{y}^{\hat{a}n}} = \sqrt{q} \left( (\beta_{si} + |\mu_{si}^{\hat{a}n}|^2) (\beta_{iu} + |\mu_{iu}^n|^2) - |\mu_{siu}^{\hat{a}n}|^2 \right). \quad (40)$$

Similarly, the auto-correlation  $R_{\bar{y}\bar{y}^{\hat{a}n}}^{\hat{a}n}$  of the observable is given by

$$R_{\bar{y}\bar{y}^{\hat{a}n}}^{\hat{a}n} = q \left( \beta_{si} + |\mu_{si}^{\hat{a}n}|^2 \right) \left( \beta_{iu} + |\mu_{iu}^{\hat{a}n}|^2 \right) + \sigma^2 + q \left( \tilde{\sigma}_{su}^{\hat{a}} \right)^2 - q |\mu_{siu}^{\hat{a}n}|^2. \quad (41)$$

Substituting the cross-correlation from (40) and the auto-correlation from (41) in (38), and simplifying further, we obtain  $\hat{g}_{siu}^{\hat{a}n}$  as stated in Lemma 1.

We next show steps involved in computing  $\tilde{\mu}_{su}^{\hat{a}}$  and  $(\tilde{\sigma}_{su}^{\hat{a}})^2$ , which in turn are required to compute  $\mathbb{E} \left( \frac{\hat{a}n}{\bar{y}} \right)$  above and the auto-correlation in (41). We first compute  $\tilde{\mu}_{su}^{\hat{a}}$  as follows. Note that  $\Re(\tilde{\mu}_{su}^{\hat{a}}) = \mathbb{E} \left( \Re(\tilde{h}_{su}^{\hat{a}}) \right) = \int_{-\infty}^{\infty} t f_{\Re(\tilde{h}_{su}^{\hat{a}})}(t) dt$ .

Since,  $\tilde{h}_{su}^{\hat{a}}$  corresponds to the error induced in estimating the channel from  $U$  to the antenna  $\hat{a}$  at  $S$ , its pdf corresponds to the pdf of the maximum of  $M$  i.i.d. Gaussian RVs each having mean zero and variance  $\tilde{\sigma}_{su}^2$ . Using this fact and results from order statistics, the pdf of  $\Re(\tilde{h}_{su}^{\hat{a}})$  is given

$$\text{by } f_{\Re(\tilde{h}_{su}^{\hat{a}})}(t) = \frac{M}{\sqrt{2\pi\tilde{\sigma}_{su}^2}} e^{-\frac{t^2}{2\tilde{\sigma}_{su}^2}} \left( 1 - Q \left( \frac{t}{\tilde{\sigma}_{su}} \right) \right)^{M-1} \quad [42].$$

Note that  $\tilde{\sigma}_{su}^2 = \frac{\beta_{su} - \gamma_{su}}{2}$ . Using this, we can write  $\Re(\tilde{\mu}_{su}^{\hat{a}}) = \frac{M}{\sqrt{2\pi\tilde{\sigma}_{su}^2}} \int_{-\infty}^{\infty} t e^{-\frac{t^2}{2\tilde{\sigma}_{su}^2}} \left( 1 - Q \left( \frac{t}{\tilde{\sigma}_{su}} \right) \right)^{M-1} dt$ . This integral can be written down as the sum of two components and simplified further by exploiting the symmetry property of Q-function [32] as

$$\Re(\tilde{\mu}_{su}^{\hat{a}}) = \frac{M}{\sqrt{2\pi\tilde{\sigma}_{su}^2}} \left( - \int_0^{\infty} t e^{-\frac{t^2}{2\tilde{\sigma}_{su}^2}} \left( Q \left( \frac{t}{\tilde{\sigma}_{su}} \right) \right)^{M-1} dt + \int_0^{\infty} t e^{-\frac{t^2}{2\tilde{\sigma}_{su}^2}} \left( 1 - Q \left( \frac{t}{\tilde{\sigma}_{su}} \right) \right)^{M-1} dt \right). \quad (42)$$

Approximating Q-function based on the identity in [43, Eqn. (14)], we obtain

$$\Re(\tilde{\mu}_{su}^{\hat{a}}) \simeq \frac{M}{\sqrt{2\pi\tilde{\sigma}_{su}^2}} \left( - \int_0^{\infty} t e^{-\frac{t^2}{2\tilde{\sigma}_{su}^2}} \left( \frac{1}{12} e^{-\frac{t^2}{2\tilde{\sigma}_{su}^2}} + \frac{1}{4} e^{-\frac{2t^2}{3\tilde{\sigma}_{su}^2}} \right)^{M-1} dt + \int_0^{\infty} t e^{-\frac{t^2}{2\tilde{\sigma}_{su}^2}} \left( 1 - \frac{1}{12} e^{-\frac{t^2}{2\tilde{\sigma}_{su}^2}} - \frac{1}{4} e^{-\frac{2t^2}{3\tilde{\sigma}_{su}^2}} \right)^{M-1} dt \right). \quad (43)$$

Using binomial expansion, and simplifying the integral further in (43), we obtain  $\Re(\tilde{\mu}_{su}^{\hat{a}})$  in simplified form as stated in (23). We know that  $\Re(\tilde{h}_{su}^{\hat{a}})$  and  $\Im(\tilde{h}_{su}^{\hat{a}})$  are identically distributed. Therefore  $\Im(\tilde{\mu}_{su}^{\hat{a}}) = \Re(\tilde{\mu}_{su}^{\hat{a}})$ . And  $\tilde{\mu}_{su}^{\hat{a}} = \Re(\tilde{\mu}_{su}^{\hat{a}}) + j\Im(\tilde{\mu}_{su}^{\hat{a}})$ .

In order to compute  $(\tilde{\sigma}_{su}^{\hat{a}})^2$ , we first compute  $\mathbb{E} \left( \Re(\tilde{h}_{su}^{\hat{a}}) \right)^2 = \int_{-\infty}^{\infty} t^2 f_{\Re(\tilde{h}_{su}^{\hat{a}})}(t) dt$ . Substituting the pdf of  $\Re(\tilde{h}_{su}^{\hat{a}})$  from above, we get  $\mathbb{E} \left( \Re(\tilde{h}_{su}^{\hat{a}}) \right)^2 = \frac{M}{\sqrt{2\pi\tilde{\sigma}_{su}^2}} \int_{-\infty}^{\infty} t^2 e^{-\frac{t^2}{2\tilde{\sigma}_{su}^2}} \left( 1 - Q \left( \frac{t}{\tilde{\sigma}_{su}} \right) \right)^{M-1} dt$ . This integral

can be written down as the sum of two components and simplified further using the symmetry property of Q-function as follows

$$\mathbb{E} \left( \Re(\tilde{h}_{su}^{\hat{a}}) \right) = \frac{M}{\sqrt{2\pi\tilde{\sigma}_{su}^2}} \left( \int_0^{\infty} t^2 e^{-\frac{t^2}{2\tilde{\sigma}_{su}^2}} \left( Q \left( \frac{t}{\tilde{\sigma}_{su}} \right) \right)^{M-1} dt + \int_0^{\infty} t^2 e^{-\frac{t^2}{2\tilde{\sigma}_{su}^2}} \left( 1 - Q \left( \frac{t}{\tilde{\sigma}_{su}} \right) \right)^{M-1} dt \right). \quad (44)$$

We next approximate Q-function based on the identity in [43, Eqn. (14)] to yield

$$\mathbb{E} \left( \Re(\tilde{h}_{su}^{\hat{a}}) \right)^2 \simeq \frac{M}{\sqrt{2\pi\tilde{\sigma}_{su}^2}} \int_0^{\infty} t^2 e^{-\frac{t^2}{2\tilde{\sigma}_{su}^2}} \times \left( \left( \frac{1}{12} e^{-\frac{t^2}{2\tilde{\sigma}_{su}^2}} + \frac{1}{4} e^{-\frac{2t^2}{3\tilde{\sigma}_{su}^2}} \right)^{M-1} + \left( 1 - \frac{1}{12} e^{-\frac{t^2}{2\tilde{\sigma}_{su}^2}} - \frac{1}{4} e^{-\frac{2t^2}{3\tilde{\sigma}_{su}^2}} \right)^{M-1} \right) dt. \quad (45)$$

Using binomial expansion to simplify (45) further and using the fact that  $\Re(\tilde{h}_{su}^{\hat{a}})$  and  $\Im(\tilde{h}_{su}^{\hat{a}})$  are i.i.d. RVs, we get  $\mathbb{E} \left( |\tilde{h}_{su}^{\hat{a}}|^2 \right)$ . Furthermore,  $(\tilde{\sigma}_{su}^{\hat{a}})^2 = \mathbb{E} \left( |\tilde{h}_{su}^{\hat{a}}|^2 \right) - |\tilde{\mu}_{su}^{\hat{a}}|^2$ , as in (24).

### C. Proof of Theorem 3

With estimated CSI, the probability of outage in WET is given by

$$\hat{P}_{\text{outage}} \simeq \Pr \left( \hat{\gamma} \left( \hat{\rho}_{su}^{\hat{a}} + \sum_{n=1}^N |\hat{g}_{siu}^{\hat{a}n}| \right)^2 \leq E_{\text{th}} \right). \quad (46)$$

Let  $\hat{X} = \hat{\rho}_{su}^{\hat{a}} = \max\{\hat{\rho}_{su}^1, \dots, \hat{\rho}_{su}^M\}$  and  $\hat{Y} = \sum_{n=1}^N |\hat{g}_{siu}^{\hat{a}n}|$ .

Thus,  $\hat{P}_{\text{outage}}$  with estimated CSI is

$$\hat{P}_{\text{outage}} \simeq \int_{\hat{y}=0}^{\infty} \Pr \left( \hat{X} \leq \hat{E}_{\text{th}} - \hat{Y} \mid \hat{Y} = \hat{y} \right) f_{\hat{Y}}(\hat{y}) d\hat{y} = \int_{\hat{y}=0}^{\hat{E}_{\text{th}}} \int_{\hat{x}=0}^{\hat{E}_{\text{th}} - \hat{y}} f_{\hat{X}}(\hat{x}) f_{\hat{Y}}(\hat{y}) d\hat{x} d\hat{y}, \quad (47)$$

where  $\hat{E}_{\text{th}} = \sqrt{\frac{E_{\text{th}}}{\hat{\gamma}}}$ ,  $f_{\hat{X}}(\hat{x})$  is the pdf of  $\hat{X}$ ,  $f_{\hat{Y}}(\hat{y})$  is the pdf of  $\hat{Y}$ . The equality in (47) follows from the fact that  $\hat{X}$  and  $\hat{Y}$  are mutually independent non-negative real RVs under the assumption that the channel estimation error,  $\tilde{h}_{su}^{\hat{a}}$  is negligibly small, which is valid for typical energy levels [3], [38]. To derive  $P_{\text{outage}}$ , we first compute  $f_{\hat{X}}(\hat{x})$  and  $f_{\hat{Y}}(\hat{y})$ . The RV  $\hat{X}$  is the maximum of  $M$  i.i.d. Rayleigh distributed RVs. Using order statistics [42], it can be shown that

$f_{\hat{X}}(\hat{x}) = \frac{2M\hat{x}}{\gamma_{su}} \left(1 - \exp\left(\frac{-\hat{x}^2}{\gamma_{su}}\right)\right)^{M-1} \exp\left(\frac{-\hat{x}^2}{\gamma_{su}}\right)$ ,  $\hat{x} \geq 0$ . To compute the pdf of  $\hat{Y}$ , we invoke CLT [35]. Based on CLT, with  $N$  large, the distribution of the sum of i.i.d. RVs approaches Gaussian distribution and its pdf is given by  $f_{\hat{Y}}(\hat{y}) = \frac{\hat{\psi}}{\sqrt{2\pi\sigma_{\hat{y}}^2}} \exp\left(\frac{-(\hat{y}-\mu_{\hat{y}})^2}{2\sigma_{\hat{y}}^2}\right)$ ,  $\hat{y} \geq 0$ , where the scaling constant  $\hat{\psi} = Q^{-1}\left(\frac{-\mu_{\hat{y}}}{\sigma_{\hat{y}}}\right)$  ensures that  $\int_0^\infty f_{\hat{Y}}(\hat{y}) d\hat{y} = 1$ .

In order to compute the mean  $\mu_{\hat{y}}$  and variance  $\sigma_{\hat{y}}^2$  above, first we model the magnitude  $|\hat{g}_{siu}^{\hat{a}n}|$  of the estimate of the cascaded channel coefficient via the  $n^{\text{th}}$  IRS element as a Rician RV [44], [45].<sup>14</sup> Thereafter, we use (38) to compute  $\mathbb{E}(\hat{g}_{siu}^{\hat{a}n}) = \mu_{siu}^{\hat{a}n}$  and  $\text{var}(\hat{g}_{siu}^{\hat{a}n}) = \left(\frac{c_1}{c_2}\right)^2 \left(\mathbb{E}\left(\left|\frac{\hat{a}n}{\bar{y}}\right|^2\right) - \left|\mathbb{E}\left(\frac{\hat{a}n}{\bar{y}}\right)\right|^2\right) = \left(\frac{c_1}{c_2}\right)^2 c_2 = \frac{c_1^2}{c_2}$  where  $c_1$  and  $c_2$  are given in Theorem 3. Based on the  $r^{\text{th}}$  moment of the Rician RV, and exploiting the fact that the terms in  $\sum_{n=1}^N |\hat{g}_{siu}^{\hat{a}n}|$  are mutually independent of each other, it can be shown that  $\mu_{\hat{y}} = \sum_{n=1}^N \mathbb{E}(|\hat{g}_{siu}^{\hat{a}n}|) = N\sqrt{\frac{c_1^2\pi}{4c_2}} L_{\frac{1}{2}}\left(\frac{-|\mu_{siu}^{\hat{a}n}|^2 c_2}{c_1^2}\right)$  and the variance,  $\sigma_{\hat{y}}^2 = \sum_{n=1}^N \text{var}(|\hat{g}_{siu}^{\hat{a}n}|) = N\left(\frac{c_1^2}{c_2} + |\mu_{siu}^{\hat{a}n}|^2 - \frac{c_1^2\pi}{4c_2} L_{\frac{1}{2}}\left(\frac{-|\mu_{siu}^{\hat{a}n}|^2 c_2}{c_1^2}\right)\right)$ . Substituting the pdf of  $\hat{X}$  and the pdf of  $\hat{Y}$  from above in (47), and simplifying using similar steps as in Appendix A, we obtain  $\hat{P}_{\text{outage}}$  in (33).

#### D. Proof of Theorem 4

To obtain diversity order of outage probability in the high transmit power regime, it suffices to analyze behavior of pdf of power gain of each of the paths from  $S$  to  $U$  near origin [46]. We first analyze pdf of the power gain of the cascaded path from  $S$  to  $U$  via the  $n^{\text{th}}$  IRS element near origin. To this end, based on Figure 2, we model  $\hat{g}_{siu}^{\hat{a}n} \sim \mathcal{CN}(\mu_{siu}^{\hat{a}n}, \nu_{siu}^{\hat{a}n})$ , where  $\mu_{siu}^{\hat{a}n} = \mathbb{E}(\hat{g}_{siu}^{\hat{a}n}) = \mu_{si}^{\hat{a}n} \mu_{iu}^{\hat{a}n}$ , and  $\nu_{siu}^{\hat{a}n} = \text{var}(\hat{g}_{siu}^{\hat{a}n}) = \frac{c_1^2}{c_2}$ . Thus, the pdf of  $|\hat{g}_{siu}^{\hat{a}n}|^2$  is given by

$$f_{|\hat{g}_{siu}^{\hat{a}n}|^2}(y) = (1 + K_{siu}) e^{-K_{siu}} e^{-(1+K_{siu})y} \times I_0\left(\sqrt{4K_{siu}(1+K_{siu})y}\right), \quad (48)$$

where  $K_{siu} = \frac{|\mu_{siu}^{\hat{a}n}|^2}{\nu_{siu}^{\hat{a}n}}$  is the corresponding Rician factor and  $I_0(\cdot)$  is modified Bessel function of the first kind [33]. Upon using the series expansion for  $\exp(-(1+K_{siu})y)$ , (48) can be expressed as

$$\begin{aligned} f_{|\hat{g}_{siu}^{\hat{a}n}|^2}(y) &= (1 + K_{siu}) e^{-K_{siu}} \left(1 + \sum_{i=1}^{\infty} \frac{(-1+K_{siu})^i y^i}{i!}\right) \\ &\times I_0\left(\sqrt{4K_{siu}(1+K_{siu})y}\right), \end{aligned} \quad (49)$$

<sup>14</sup>Based on Figure 2, we see that modeling the magnitude of cascaded channel coefficient as a Rician RV is fairly accurate.

The pdf in (49) can be approximated as a single polynomial near the origin and

$$\lim_{y \rightarrow 0} f_{|\hat{g}_{siu}^{\hat{a}n}|^2}(y) = b_{siu} y^{t_{siu}} + O(y^{t_{siu}+\epsilon}), \quad (50)$$

where  $b_{siu}$  is a constant, the parameter  $t_{siu}$  captures the diversity order of the outage probability,  $O(\cdot)$  denotes the big  $O$  notation and  $\epsilon > 0$ . Comparing (49) with (50) at  $y \rightarrow 0$ , we obtain  $b_{siu} = (1 + K_{siu}) \exp(-K_{siu})$  and  $t_{siu} = 0$ . Using (50), the probability of outage in WET due the cascaded path via  $n^{\text{th}}$  IRS element is given by

$$\begin{aligned} p_{\text{outage}}^{\hat{a}n} &= \int_0^{\frac{p_{\text{th}}}{p}} (b_{siu} y^{t_{siu}} + O(y^{t_{siu}+\epsilon})) dy \\ &= \frac{b_{siu}}{t_{siu}+1} \left(\frac{p_{\text{th}}}{p}\right)^{t_{siu}+1} + O\left(\left(\frac{p_{\text{th}}}{p}\right)^{t_{siu}+1+\epsilon}\right), \end{aligned} \quad (51)$$

where  $p_{\text{th}} = \frac{E_{\text{th}}}{\eta_r(\tau_c - (M+N)\tau_p)}$  denotes the threshold power required at the user. Neglecting the higher order terms in (51), we can see that the outage probability due to the reflected path via the  $n^{\text{th}}$  IRS element decays as  $p^{-(t_{siu}+1)} = p^{-1}$ . Since, there are  $N$  independent cascaded paths from  $S$  to  $U$  via the IRS, the total contribution to the diversity order in outage probability due to the  $N$ -element IRS equals  $N$  [46].

Furthermore, the pdf of channel power gain from the strongest antenna at  $S$  to  $U$  is given by

$$\begin{aligned} f_{|\hat{h}_{su}^{\hat{a}}|^2}(x) &= \frac{2M}{\gamma_{su}} \left(1 - e^{-\frac{2x}{\gamma_{su}}}\right)^{M-1} e^{-\frac{2x}{\gamma_{su}}}, \\ &= \frac{2M}{\gamma_{su}} \left(-\sum_{i=1}^{\infty} \left(\frac{-2}{\gamma_{su}}\right)^i \frac{x^i}{i!}\right)^{M-1} \left(\sum_{i=0}^{\infty} \left(\frac{-2}{\gamma_{su}}\right)^i \frac{x^i}{i!}\right), \end{aligned} \quad (52)$$

where (52) is obtained by writing the series expansion for  $\exp\left(\frac{-2x}{\gamma_{su}}\right)$ . By writing the pdf in (52) as a single polynomial near the origin, we get

$$\lim_{x \rightarrow 0} f_{|\hat{h}_{su}^{\hat{a}}|^2}(x) = b_{su} x^{t_{su}} + O(x^{t_{su}+\epsilon}), \quad (53)$$

where  $b_{su}$  is a constant and the parameter  $t_{su}$  captures the diversity order of the outage probability. Comparing (52) and (53) at  $x \rightarrow 0$ , we obtain  $b_{su} = \frac{4M}{\gamma_{su}^2}$  and  $t_{su} = M - 1$ . Using (53), the probability of outage in WET due to the direct path is given by

$$\begin{aligned} p_{\text{outage}}^{\hat{a}} &= \int_0^{\frac{p_{\text{th}}}{p}} (b_{su} x^{t_{su}} + O(x^{t_{su}+\epsilon})) dx \\ &= \frac{b_{su}}{t_{su}+1} \left(\frac{p_{\text{th}}}{p}\right)^{t_{su}+1} + O\left(\left(\frac{p_{\text{th}}}{p}\right)^{t_{su}+1+\epsilon}\right). \end{aligned} \quad (54)$$

Neglecting the higher order terms in (54), we can see that the outage probability due to the direct path decays as  $p^{-(t_{su}+1)} = p^{-M}$ . Since this path from the strongest antenna at  $S$  to  $U$  is independent of every cascaded path from  $S$  to  $U$  via the IRS elements, the total diversity order of outage probability is equal to  $M + N$  [46].

## REFERENCES

- [1] T. Barnett Jr., S. Jain, U. Andra, and T. Khurana, "Cisco visual networking index (VNI) complete forecast update, 2017–2022," CKN Presentation, Cisco, Los Angeles, CA, USA, 2018.
- [2] Z. Popović, E. A. Falkenstein, D. Costinett, and R. Zane, "Low-power far-field wireless powering for wireless sensors," *Proc. IEEE*, vol. 101, no. 6, pp. 1397–1409, Jun. 2013.
- [3] S. Kashyap, E. Björnson, and E. G. Larsson, "On the feasibility of wireless energy transfer using massive antenna arrays," *IEEE Trans. Wireless Commun.*, vol. 15, no. 5, pp. 3466–3480, May 2016.
- [4] M. K. Sarangi and S. Kashyap, "Impact of pilot allocation strategies on outage in wireless energy transfer using massive antenna arrays," *IEEE Trans. Wireless Commun.*, vol. 20, no. 2, pp. 942–954, Feb. 2021.
- [5] D. Mishra and H. Johansson, "Channel estimation and low-complexity beamforming design for passive intelligent surface assisted MISO wireless energy transfer," in *Proc. IEEE Int. Conf. Acoust., Speech Signal Process. (ICASSP)*, Apr. 2019, pp. 4659–4663.
- [6] D. Mishra and E. G. Larsson, "Passive intelligent surface assisted MIMO powered sustainable IoT," in *Proc. IEEE Int. Conf. Acoust., Speech Signal Process. (ICASSP)*, May 2020, pp. 8961–8965.
- [7] Q. Wu, S. Zhang, B. Zheng, C. You, and R. Zhang, "Intelligent reflecting surface-aided wireless communications: A tutorial," *IEEE Trans. Commun.*, vol. 69, no. 5, pp. 3313–3351, May 2021.
- [8] O. Özdoğan, E. Björnson, and E. G. Larsson, "Intelligent reflecting surfaces: Physics, propagation, and pathloss modeling," *IEEE Wireless Commun. Lett.*, vol. 9, no. 5, pp. 581–585, May 2020.
- [9] F. E. Bouanani, S. Muhaidat, P. C. Sofotasios, O. A. Dobre, and O. S. Badarneh, "Performance analysis of intelligent reflecting surface aided wireless networks with wireless power transfer," *IEEE Commun. Lett.*, vol. 25, no. 3, pp. 793–797, Mar. 2021.
- [10] L. Zhao, Z. Wang, and X. Wang, "Wireless power transfer empowered by reconfigurable intelligent surfaces," *IEEE Syst. J.*, vol. 15, no. 2, pp. 2121–2124, Jun. 2021.
- [11] H. Yang, X. Yuan, J. Fang, and Y.-C. Liang, "Reconfigurable intelligent surface aided constant-envelope wireless power transfer," *IEEE Trans. Signal Process.*, vol. 69, pp. 1347–1361, 2021.
- [12] Z. Feng, B. Clerckx, and Y. Zhao, "Waveform and beamforming design for intelligent reflecting surface aided wireless power transfer: Single-user and multi-user solutions," *IEEE Trans. Wireless Commun.*, early access, Jan. 10, 2022, doi: [10.1109/TWC.2021.3139440](https://doi.org/10.1109/TWC.2021.3139440).
- [13] Y. Zheng, S. Bi, Y. J. Zhang, Z. Quan, and H. Wang, "Intelligent reflecting surface enhanced user cooperation in wireless powered communication networks," *IEEE Wireless Commun. Lett.*, vol. 9, no. 6, pp. 901–905, Jun. 2020.
- [14] D. Xu, V. Jamali, X. Yu, D. W. K. Ng, and R. Schober, "Optimal resource allocation design for large IRS-assisted SWIPT systems: A scalable optimization framework," *IEEE Trans. Commun.*, vol. 70, no. 2, pp. 1423–1441, Feb. 2022.
- [15] Q. Wu and R. Zhang, "Joint active and passive beamforming optimization for intelligent reflecting surface assisted SWIPT under QoS constraints," *IEEE J. Sel. Areas Commun.*, vol. 38, no. 8, pp. 1735–1748, Aug. 2020.
- [16] S. Zargari, A. Khalili, and R. Zhang, "Energy efficiency maximization via joint active and passive beamforming design for multiuser MISO IRS-aided SWIPT," *IEEE Wireless Commun. Lett.*, vol. 10, no. 3, pp. 557–561, Mar. 2021.
- [17] R. Sarvendranath and A. K. R. Chavva, "Low-complexity joint antenna selection and beamforming for an IRS assisted system," in *Proc. IEEE Wireless Commun. Netw. Conf. (WCNC)*, Apr. 2021, pp. 1–6.
- [18] Z. Abdullah, G. Chen, S. Lambotaran, and J. A. Chambers, "Low-complexity antenna selection and discrete phase-shifts design in IRS-assisted multiuser massive MIMO networks," *IEEE Trans. Veh. Technol.*, vol. 71, no. 4, pp. 3980–3994, Apr. 2022.
- [19] J. He, K. Yu, Y. Shi, Y. Zhou, W. Chen, and K. B. Letaief, "Reconfigurable intelligent surface assisted massive MIMO with antenna selection," *IEEE Trans. Wireless Commun.*, early access, Dec. 17, 2021, doi: [10.1109/TWC.2021.3133272](https://doi.org/10.1109/TWC.2021.3133272).
- [20] X. Lu, I. Flint, D. Niyato, N. Privault, and P. Wang, "Self-sustainable communications with RF energy harvesting: Ginibre point process modeling and analysis," *IEEE J. Sel. Areas Commun.*, vol. 34, no. 5, pp. 1518–1535, May 2016.
- [21] Z. Yang, Z. Ding, P. Fan, and G. K. Karagiannidis, "Outage performance of cognitive relay networks with wireless information and power transfer," *IEEE Trans. Veh. Technol.*, vol. 65, no. 5, pp. 3828–3833, May 2016.
- [22] A. N. Abdulfattah, C. C. Tsimenidis, B. Z. Al-Jewad, and A. Yakovlev, "Performance analysis of MICS-based RF wireless power transfer system for implantable medical devices," *IEEE Access*, vol. 7, pp. 11775–11784, 2019.
- [23] M. Najafi, V. Jamali, R. Schober, and H. V. Poor, "Physics-based modeling and scalable optimization of large intelligent reflecting surfaces," *IEEE Trans. Commun.*, vol. 69, no. 4, pp. 2673–2691, Apr. 2021.
- [24] X. Pei *et al.*, "RIS-aided wireless communications: Prototyping, adaptive beamforming, and indoor/outdoor field trials," *IEEE Trans. Commun.*, vol. 69, no. 12, pp. 8627–8640, Dec. 2021.
- [25] Q. Wu and R. Zhang, "Intelligent reflecting surface enhanced wireless network: Joint active and passive beamforming design," in *Proc. IEEE Global Commun. Conf. (GLOBECOM)*, Dec. 2018, pp. 1–6.
- [26] Q.-U.-A. Nadeem, H. Alwazani, A. Kammoun, A. Chaaban, M. Debbah, and M.-S. Alouini, "Intelligent reflecting surface-assisted multi-user MISO communication: Channel estimation and beamforming design," *IEEE Open J. Commun. Soc.*, vol. 1, pp. 661–680, 2020.
- [27] T. L. Jensen and E. De Carvalho, "An optimal channel estimation scheme for intelligent reflecting surfaces based on a minimum variance unbiased estimator," in *Proc. IEEE Int. Conf. Acoust., Speech Signal Process. (ICASSP)*, May 2020, pp. 5000–5004.
- [28] H. Shen, W. Xu, S. Gong, C. Zhao, and D. W. K. Ng, "Beamforming optimization for IRS-aided communications with transceiver hardware impairments," *IEEE Trans. Commun.*, vol. 69, no. 2, pp. 1214–1227, Feb. 2021.
- [29] J.-M. Kang, I.-M. Kim, and D. I. Kim, "Joint Tx power allocation and Rx power splitting for SWIPT system with multiple nonlinear energy harvesting circuits," *IEEE Wireless Commun. Lett.*, vol. 8, no. 1, pp. 53–56, Feb. 2019.
- [30] M. A. Abouzied, K. Ravichandran, and E. Sánchez-Sinencio, "A fully integrated reconfigurable self-startup RF energy-harvesting system with storage capability," *IEEE J. Solid-State Circuits*, vol. 52, no. 3, pp. 704–719, Mar. 2017.
- [31] Y. Zeng and R. Zhang, "Optimized training design for wireless energy transfer," *IEEE Trans. Commun.*, vol. 63, no. 2, pp. 536–550, Feb. 2015.
- [32] M. Simon and M.-S. Alouini, *Digital Communication Over Fading Channels*. 2nd ed. Hoboken, NJ, USA: Wiley, 2005.
- [33] I. S. Gradshteyn and I. M. Ryzhik, *Table of Integrals, Series and Products*, 4th ed. New York, NY, USA: Academic, 1980.
- [34] Q. Tao, J. Wang, and C. Zhong, "Performance analysis of intelligent reflecting surface aided communication systems," *IEEE Commun. Lett.*, vol. 24, no. 11, pp. 2464–2468, Nov. 2020.
- [35] A. Papoulis, *Probability, Random Variables and Stochastic Processes*. 3rd ed. New York, NY, USA: McGraw-Hill, 1991.
- [36] M. Fréchet, "Généralisation du théorème des probabilités totales," *Fundamenta Mathematicae*, vol. 25, no. 1, pp. 379–387, 1935.
- [37] S. M. Kay, *Fundamentals of Statistical Signal Processing: Estimation Theory*, vol. 1, 1st ed. Upper Saddle River, NJ, USA: Prentice-Hall, 1993.
- [38] T. A. Khan, A. Yazdan, and R. W. Heath, Jr., "Optimization of power transfer efficiency and energy efficiency for wireless-powered systems with massive MIMO," *IEEE Trans. Wireless Commun.*, vol. 17, no. 11, pp. 7159–7172, Nov. 2018.
- [39] E. Björnson, O. Özdoğan, and E. G. Larsson, "Intelligent reflecting surface versus decode-and-forward: How large surfaces are needed to beat relaying?" *IEEE Wireless Commun. Lett.*, vol. 9, no. 2, pp. 244–248, Feb. 2020.
- [40] P. Wang, J. Fang, H. Duan, and H. Li, "Compressed channel estimation for intelligent reflecting surface-assisted millimeter wave systems," *IEEE Signal Process. Lett.*, vol. 27, pp. 905–909, 2020.
- [41] Y. Yang, B. Zheng, S. Zhang, and R. Zhang, "Intelligent reflecting surface meets OFDM: Protocol design and rate maximization," *IEEE Trans. Commun.*, vol. 68, no. 7, pp. 4522–4535, Jul. 2020.
- [42] H. A. David and H. N. Nagaraja, *Order Statistics*. 3rd ed. Hoboken, NJ, USA: Wiley, 2003.
- [43] M. Chiani, D. Dardari, and M. K. Simon, "New exponential bounds and approximations for the computation of error probability in fading channels," *IEEE Trans. Wireless Commun.*, vol. 2, no. 4, pp. 840–845, Jul. 2003.
- [44] S. Bharadwaj and N. B. Mehta, "Accurate performance analysis of single and opportunistic AF relay cooperation with imperfect cascaded channel estimates," *IEEE Trans. Commun.*, vol. 61, no. 5, pp. 1764–1775, May 2013.
- [45] C. S. Patel and G. L. Stuber, "Channel estimation for amplify and forward relay based cooperation diversity systems," *IEEE Trans. Wireless Commun.*, vol. 6, no. 6, pp. 2348–2356, Jun. 2007.
- [46] Z. Wang and G. B. Giannakis, "A simple and general parameterization quantifying performance in fading channels," *IEEE Trans. Commun.*, vol. 51, no. 8, pp. 1389–1398, Aug. 2003.



**Chandan Kumar** (Student Member, IEEE) received the Bachelor of Technology degree in electronics and communication engineering from the Bihar Institute of Technology (BIT), Sindri, India, in 2011. He is currently pursuing the Ph.D. degree with the Indian Institute of Technology (IIT), Guwahati, India. He was a Test Engineer with Infosys Ltd., Bengaluru, India, from 2011 to 2013. During his Ph.D., he worked on research problems related to massive MIMO, intelligent reflecting surface (IRS) aided communication, wireless information, and energy transfer in sensor networks.



**Salil Kashyap** (Member, IEEE) received the Ph.D. degree in electrical communication engineering from the Indian Institute of Science (IISc), Bengaluru, India, in 2014. He was a Senior DSP Engineer with Marvell from 2016 to 2017, where he designed physical-layer algorithms for next-generation WLANs (IEEE 802.11ax) and a Post-Doctoral Researcher with the Division of Communication Systems, Linköping University, Sweden, from 2014 to 2016. In 2017, he joined the IIT Guwahati, where he is currently an Assistant Professor with the Department of Electronics and Electrical Engineering. His research interests include modeling, performance analysis, resource allocation, and algorithm design for 5G and beyond 5G communication systems, including intelligent reflecting surfaces, massive MIMO, NOMA, OFDM, cognitive radio, and wireless energy transfer.



**Rimalapudi Sarvendranath** (Member, IEEE) received the Bachelor of Technology degree in electrical and electronics engineering from the National Institute of Technology Karnataka, Surathkal, in 2009, and the Master of Engineering and Ph.D. degrees from the Department of Electrical Communication Engineering (ECE), Indian Institute of Science (IISc), Bengaluru, India, in 2012 and 2020, respectively. From 2009 to 2010, he was a Research Assistant with the Department of Instrumentation, IISc, where he was involved in the development of image processing algorithms. From 2012 to 2016, he was with Broadcom Communications Technologies Pvt. Ltd., Bengaluru, where he worked on the development and implementation of algorithms for LTE and IEEE 802.11ac wireless standards. In 2021, he was a Post-Doctoral Researcher with the Department of Electrical Engineering (ISY), Linköping University, Sweden. He is currently working as an Assistant Professor with the EEE Department, Indian Institute of Technology Guwahati. His research interests include wireless communications, multiple antenna techniques, spectrum sharing, and next-generation wireless standards.



**Supreet Kumar Sharma** received the Bachelor of Technology degree in electrical and electronics engineering from the Maharaja Agrasen Institute of Technology, Delhi, India, in 2016, and the M.Tech. degree in communication engineering from the Indian Institute of Technology (IIT) Guwahati, India, in 2020. He is currently with Mavenir Systems Pvt. Ltd., Bengaluru, India, working on the design and development for next-generation mobile network infrastructure designed with cloud-native virtualization techniques. He has gained hands on experience on 5G/NR L3 stack development in CallProcessing, RRC, F1AP, E1AP, and NGAP protocols. His research interests include design and analysis of algorithms for wireless networks and resource allocation.